nature medicine

Article

https://doi.org/10.1038/s41591-026-04704-z

Extended follow-up of in vivo BCMA CAR-T therapy in relapsed/refractory multiple myeloma

Received: 27 March 2026

Accepted: 7 September 2026

Published online: 06 October 2026

Check for updates

A list of authors and their affiliations appears at the end of the paper

Data on long-term outcomes of in vivo chimeric antigen receptor T cell (CAR-T) therapy remain scarce. We previously reported preliminary safety and efficacy data of in vivo B-cell maturation antigen (BCMA) CAR-T (ESO-T01), in four patients with relapsed/refractory multiple myeloma, without leukapheresis and lymphodepletion, with up to 3 months of follow-up. The primary endpoints included safety and tolerability, while the secondary endpoints comprised efficacy, pharmacokinetics and pharmacodynamics. All patients developed dual-phase cytokine release syndrome (grades 1–3) and hematotoxicities (grade ≥3). One patient developed grade 1 immune effector cell-associated neurotoxicity syndrome. The objective response rate reached 100% (two stringent complete response and two partial response). Here we update the data on long-term safety and response durability with a maximal follow-up of 15 months. No immunogenicity- or integration-related toxicities occurred, and no important adverse events related to ESO-T01 emerged beyond the initial report. Of the four patients, one maintained stringent complete response for 15 months. The median progression-free survival was 4.0 (range 3.0–15.0) months. After progression, diverse salvage therapies extended overall survival to 5.5–10.9 months after infusion. Three patients experienced relapse or progression, all with extramedullary involvement, and eventually died during follow-up. One patient achieved durable response with robust expansion from ex vivo CAR-T. Collectively, these updated results provide additional insights on the safety and efficacy of in vivo CAR-T therapies. The limited persistence observed necessitates the further optimization of the in vivo CAR-T platform. ClinicalTrials.gov identifier: NCT06691685.

Chimeric antigen receptor T cell (CAR-T) therapy has revolutionized the landscape of immunotherapy. However, availability is substantially constrained by manufacturing limitations, logistical demands, long waiting time and prohibitive costs[1]. According to a real-world study in the USA, among patients with relapsed or refractory multiple myeloma (R/R MM) listed for commercial B-cell maturation antigen (BCMA) CAR-T therapy, the 12-month cumulative incidence of receiving CAR-T therapy was less than 40%, and the mortality while waiting for treatment reached 26% (ref. 2). In vivo CAR technology leverages viral or nonviral vectors to deliver CAR directly to endogenous T cells within the human body, offering a promising alternative and transforming CAR-T from a personalized, customized product into an accessible, off-the-shelf therapeutic modality[3,4]. Over the past 5 years, preclinical research in this area has advanced rapidly[5–8], catalyzing a growing number of registered clinical trials. Nevertheless, clinical data still remain very scarce.

e-mail: dr_huyu@126.com; hmei@hust.edu.cn

https://doi.org/10.1038/s41591-026-04704-z

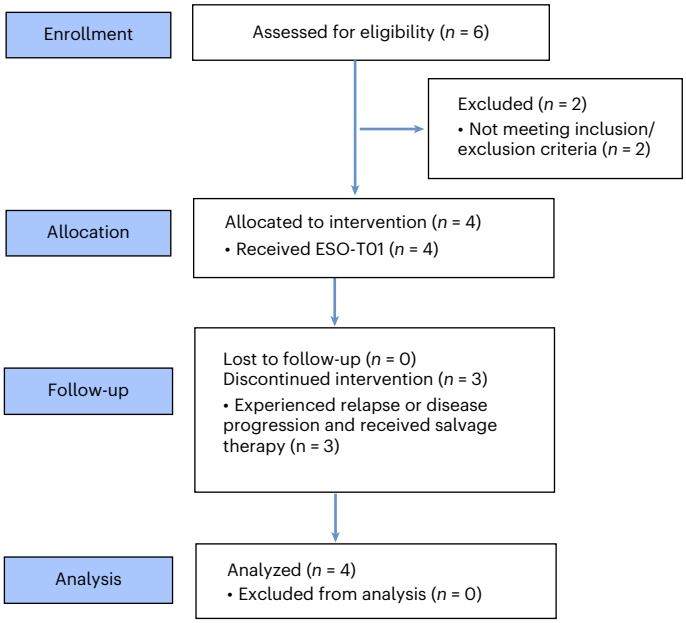


Fig. 1 | CONSORT patient flow diagram. Patient disposition at the data cutoff of March 2026.

We previously reported the first-in-human clinical study of ESO-T01, an in vivo BCMA-targeted CAR-T therapy for MM[9]. Subsequently, Wang et al.[10] published clinical results using HN2301, a lipid nanoparticle delivering an anti-CD19 CAR for systemic lupus erythematosus. Five patients receiving 1–3 infusions of HN2301 demonstrated a decrease in disease activity 3 months after infusion. More recently, Kelonia published preliminary clinical data for KLN-1010, a lentiviral vector encapsulating a BCMA-directed CAR[11]. All patients with R/R MM attained objective responses after the treatment. These early results highlight the potential of in vivo CAR-T therapy to overcome existing barriers and broaden the applicability of CAR-T across a range of diseases. While initial efficacy has been demonstrated in these early-phase trials, extended follow-up data are essential to fully address safety and durability concerns. Following the acquisition of EsoBiotec by AstraZeneca, the ESO-T01 clinical trial was discontinued. Here we report the follow-up of four patients with MM treated with ESO-T01. Baseline characteristics and initial treatment details have been previously published[9]. In this report, we focus on the long-term clinical outcomes, safety profile and subsequent treatments following disease relapse or progression. These data are critical for understanding the durability of response and provide valuable insights into the long-term management of patients receiving in vivo CAR-T therapy. By documenting these findings, we aim to inform future clinical practices for similar patient populations and contribute to the ongoing optimization of in vivo CAR-T platforms.

Results

Patients and clinical outcomes

From November 2024 to February 2025, six patients with R/R MM were screened. Two individuals (both screened in February 2025) did not meet the inclusion or exclusion criteria and were excluded. Ultimately, four patients were enrolled and treated with ESO-T01 (Fig. 1). The first patient was enrolled on 19 November 2024 and the last patient on 17 January 2025. Baseline characteristics are summarized in Table 1. The median age was 63 years, and half of the patients were male. All patients had received a median of four prior treatment lines. One patient had penta-refractory disease, and another had previously received BCMA-GPRC5D CAR-T before screening. Four patients had extramedullary disease, two of whom presented with multiple lesions. All four patients had bulky plasmacytoma with a diameter exceeding 5 cm. ESO-T01 was intravenously administrated at a single dose of 0.2×10^9 transduction units, without leukapheresis and lymphodepletion. All participants experienced vector-related reactions. The most common manifestations were fever, hypoxemia and hypotension, which corresponded to grades 1–3 cytokine release syndrome (CRS). Self-limiting neurotoxicities occurred in Patient 1 within 24 h after infusion. During the CAR-T cell expansion phase, all patients developed grade 1 CRS, and Patient 4 developed grade 1 immune effector cell-associated neurotoxicity syndrome (ICANS). All adverse events were well controlled (Extended Data Fig. 1a). Grade 3 to 4 hematotoxicities occurred in all patients, including neutropenia (75%), leukopenia (50%), thrombocytopenia (50%) and lymphopenia (75%). By 1 month, three out of the four patients had recovered to hematologic toxicity of grade ≤2. The remaining patient, who continued to exhibit grade 3 neutropenia, had already presented with grade 3 neutropenia at baseline. Most hematotoxicities resolved to baseline or better during follow-up.

As of the data cutoff in March 2026, the longest follow-up had reached 15 months following ESO-T01 infusion. After treatment, two patients achieved a stringent complete response (sCR), and the other two achieved a partial response (PR). Notably, one patient had accomplished 15 months of follow-up with a sustained sCR. However, the durability of remission was unfavorable in the remaining patients with high baseline tumor burden, including those presenting cerebral spinal fluid (CSF) involvement and multiple extramedullary disease. Three patients relapsed or progressed at 5, 3 and 3 months after infusion (Fig. 2a), respectively. Despite receiving salvage therapies, including chemotherapy in two patients and BCMA-GPRC5D bispecific CAR-T in one patient, all three eventually died of infection, disease progression and intracranial hemorrhage, respectively (Fig. 2a and Extended Data Fig. 1b). The CAR-T kinetics indicated that in Patients 1 and 3, relapse and disease progression occurred when CAR-T cells became undetectable (Fig. 2b). However, in Patient 4, despite a persistent presence of CAR-T cells in the CSF (Extended Data Fig. 2), they were unable to completely eradicate the MM cells. By the third month, tumor cells in the CSF had substantially increased and the patient experienced disease progression.

Individual patient outcomes during follow-up

Patient 1 had penta-refractory disease before the treatment, characterized by high tumor burden, extensive extramedullary disease, large mass (11.6 × 3.3 cm) and central nervous system involvement. After ESO-T01 treatment, the patient achieved sCR in month 2 and increased quality of life. However, in month 4, the patient developed a facial swelling. In month 5, the positron emission tomography-computed tomography revealed an extramedullary relapse (Extended Data Fig. 3a), including involvement of the CSF (94% of nucleated cells). He then received one cycle of aponermin, thalidomide and dexamethasone and one cycle of DT-PACE (dexamethasone, thalidomide, platinol cisplatin, adriamycin doxorubicin, cyclophosphamide, etoposide). During the chemotherapy, he suffered a severe pulmonary infection. The next-generation sequencing suggested a mixed infection with a variety of bacteria and fungi, which were all opportunistic pathogens. Though we immediately adjusted the antibiotics based on drug resistance profiles, the infection ultimately led to respiratory failure and death. This occurred 8.1 months after he received in vivo CAR-T therapy.

Patient 2 had the lowest tumor burden at baseline with only two paraskeletal lesions. After ESO-T01 infusion, she developed grade 1 CRS characterized by fever on day 9 accompanied by mild elevation of inflammatory markers. The lesions regressed rapidly, and a biopsy taken on day 10 revealed marked infiltration of $CD3^+$ T cells, which were confirmed to incorporate CAR-T cells by flow cytometry and quantitative polymerase chain reaction (qPCR)[4]. During the expansion phase, her CAR-T cells exhibited a predominantly naive and central memory

https://doi.org/10.1038/s41591-026-04704-z

Table 1 | Patient characteristics

Characteristics	Patient 1	Patient 2	Patient 3	Patient 4
Age (years)	69	40	67	59
Sex	Male	Female	Female	Male
Eastern Cooperative Oncology Group status	2	0	1	1
Monoclonal type	κ light chain	κ light chain	λ light chain	IgG-λ
Time since diagnosis (months)	36	19	14	16
Revised International Staging System stage	III	I	II	II
Durie–Salmon staging	IIIA	IIIA	IIIA	IIIA
Abnormal cytogenetics	Negative	Negative	Negative	t(4;14), amp (1q21)
Disease characteristics	Refractory	Relapsed	Refractory	Refractory
Underlying diseases	Chronic bronchitis	Hypothyroidism	Hypertension	-
Extramedullary disease	Yes	Yes	Yes	Yes
Maximum measurable lesion (cm)	11.6×3.3	5.5×5.2	9.3×6.4	7.1×3.7
Prior treatment lines	4	2	4	4
Prior proteasome inhibitors	Yes	Yes	Yes	Yes
Prior immunomodulatory drug	Yes	Yes	Yes	Yes
Prior anti-CD38 monoclonal antibody	Yes	No	Yes	Yes
Prior autologous stem cell transplantation	No	Yes	No	No
Prior CAR-T	No	No	No	Yes
Time between screening and infusion (days)	8	3	11	5

phenotype, potentially explaining their long-term persistence[9]. At month 3, a slight increase in CAR-T cells was detected by qPCR, though not by flow cytometry (Fig. 2b). She has now accomplished 15 months of follow-up, and still maintained sCR (Extended Data Fig. 3b).

Patient 3 presented with multiple extramedullary lesions at baseline. Though with unfavorable CAR-T cell expansion, she achieved PR 1 month after ESO-T01 infusion. Disease progression occurred at month 3, characterized by diffuse lesions throughout the body (Extended Data Fig. 3c). The recurrent myeloma cells can also be detected in her CSF, accounting for 95.67% of nucleated cells. Since the biopsies of bone marrow and subcutaneous mass in left posterior lumbar revealed 0% and 50% positivity of BCMA expression on tumor cells (Extended Data Fig. 3d), respectively, leukapheresis was promptly performed to manufacture BCMA-GPRC5D bispecific CAR-T cells. Subsequently, one cycle of bridging therapy with aponermin, pomalidomide and dexamethasone was administered. Four months after the initial treatment with ESO-T01, the patient received an infusion of these CAR-T cells at a dose of 1.5×10^6 cells per kg following lymphodepleting chemotherapy (Fig. 2c). Intermittent intrathecal therapy with methotrexate, cytarabine and dexamethasone was administered for CSF involvement. One month after infusion, all myeloma-related biochemical indicators had normalized or turned negative (Fig. 2d). Further, the patient achieved tumor clearance in the bone marrow, along with marked regression of numerous extramedullary lesions (Fig. 2e), culminating in a very good partial response (VGPR). As for the treatment-related toxicities, the patient developed high fever on day 2 and recurrent fever on day 20, with prolonged hypotension lasting until day 23, which was defined as grade 3 CRS. Grade 1 ICANS occurred from day 5 to day 14. These syndromes were then controlled by glucocorticoids, anakinra, norepinephrine and other symptomatic therapies (Extended Data Fig. 1b). However, on day 27, 4 days after CRS resolution, the patient developed immune effector cell-associated hemophagocytic lymphohistiocytosis-like syndrome, characterized by fever (Extended Data Fig. 3e), elevated ferritin (Fig. 2c) and soluble CD25 (6473 U ml^{-1}), impaired NK cell cytotoxicity (cytoplasmic perforin 69.15% and cytoplasmic granzyme 63.83%), grade 4 cytopenia (Fig. 2c), and hemophagocytes on bone marrow smear. Despite treatment with corticosteroids, anakinra, ruxolitinib, persistent platelet transfusion support and even plasma exchange, she experienced acute disturbance of consciousness due to intracranial hemorrhage on day 32 and died 3 days later (Extended Data Fig. 1b). Notably, the initial in vivo CAR-T cells peaked on day 10, with a maximum concentration of 86 cells per µl by flow cytometry and 6,600 copies per µg of genomic DNA (gDNA) by digital droplet digital droplet polymerase chain reaction (ddPCR), while the ex vivo CAR-T cells peaked on day 16, reaching a maximum concentration of 419 cells per µl and 155,500 copies per µg of gDNA (Fig. 2c). Ex vivo CAR-T also demonstrated a dual-peak expansion (Fig. 2c), which may be associated with the occurrence of immune effector cell-associated hemophagocytic lymphohistiocytosis-like syndrome[12]. Moreover, in the BCMA-GPRC5D CAR-T infused product, $CD4^+$ T cells constituted a larger proportion, and CAR^+ cells exhibited higher percentages of central memory T cell (T_{CM}) and naive T cell (T_n) phenotypes compared to the CAR^- population (Fig. 2f). However, at the expansion peak of ex vivo CAR-T cells, $CD8^+$ T cells accounted for a predominant proportion, with nearly 99% being effector T cells, while senescent phenotype ($CD28^-CD57^+$) comprised only 4.4% (Fig. 2f). In contrast, during the expansion peak after her prior in vivo CAR-T therapy, though effector cells also constituted a high proportion, senescent T cells accounted for as much as 72.2% of CAR^+ T cells[9]. These differences may partially explain the improved efficacy of the second ex vivo CAR-T therapy over the first in vivo one.

Patient 4 had previously failed the ex vivo BCMA-GPRC5D CAR-T therapy before receiving in vivo CAR-T, but maintained 100% positivity of BCMA expression in bone marrow myeloma cells. Further, he had a high tumor burden in the CSF. His best response to ESO-T01 was PR. In the second month after infusion, tumor cells remained detectable in the CSF, and increased by the third month, accounting for 98.78% of nucleated cells. Although the M protein declined from 5.2 g l^{-1} in month 2 to 4.1 g l^{-1} in month 3, positron emission tomography-computed tomography at this time revealed a new lesion with abnormally increased metabolism in the left parietal-occipital junction, accompanied by surrounding edema and ill-defined margins. The pre-existing lesions

https://doi.org/10.1038/s41591-026-04704-z

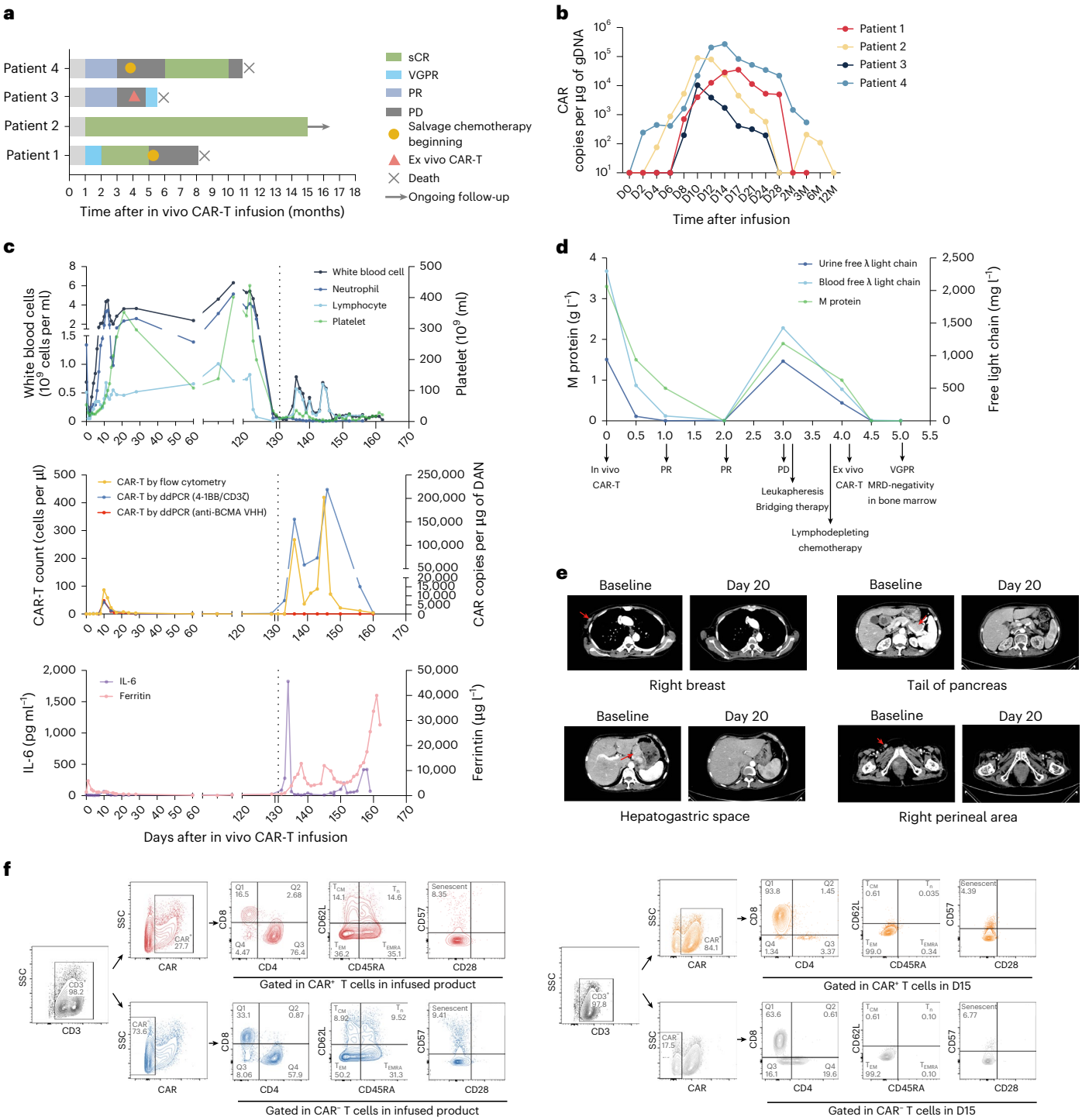


Fig. 2 | Clinical outcomes of four patients treated with in vivo CAR-T therapy. **a**, Swimmer's plot of four patients following ESO-T01 infusion. Patient 3 received BCMA-GPRC5D ex vivo CAR-T therapy 4 months after infusion. **b**, CAR transgene copy numbers in peripheral blood of four patients following ESO-T01 treatment by ddPCR. **c**, Longitudinal trajectory of white blood cells, lymphocyte, neutrophil, CAR-T, interleukin-6 (IL-6) and ferritin of Patient 3 during treatment with a comparison of in vivo and ex vivo CAR-T therapy. The dashed line denotes the time point of ex vivo BCMA-GPRC5D CAR-T infusion. **d**, Change of M protein and free light chain of Patient 3 during the treatment of in vivo and ex vivo CAR-T therapy. **e**, Imaging results of Patient 3 before and after treatment with BCMA-GPRC5D CAR-T therapy. **f**, Phenotype of T cells in the infused product of BCMA-GPRC5D CAR-T and at the expansion peak (day 15) of Patient 3 after ex vivo CAR-T treatment. D, days; M, months; SSC, side scatter; T_{EM}, effector memory T cell; T_{EMRA}, T effector memory cells re-expressing CD45RA.

also showed elevated metabolic activity (Extended Data Fig. 3f). These findings suggested disease progression. This patient then began to receive chemotherapy with the CPT-XKd (selinexor, carfilzomib and dexamethasone) regimen for four cycles. Throughout this period, intermittent lumbar punctures and intrathecal administration of methotrexate, cytarabine and dexamethasone were also performed. Evaluation after chemotherapy confirmed sCR with negative minimal residual disease (MRD) in the CSF. The patient then underwent maintenance therapy with pomalidomide and carfilzomib. However, his disease relapsed in the central nervous system 4 months later and

was refractory to subsequent salvage therapy, ultimately succumbing to progressive disease (PD) 10.9 months after the ESO-T01 treatment.

Adverse events and immune reconstitution following in vivo CAR-T treatment

The safety profiles of the four patients were manageable, with most adverse events returning to baseline or resolving within 2 to 3 months after infusion (Fig. 3a). Hypogammaglobulinemia was observed in all patients except Patient 4 (Fig. 3a and Extended Data Fig. 4a), whose IgG levels could not be accurately assessed due to predominant tumor-derived production. Notably, this patient also demonstrated persistent low levels of IgA and IgM throughout follow-up (Extended Data Fig. 4a). Given that hypogammaglobulinemia is a common adverse event following BCMA-targeted therapy, intermittent immunoglobulin infusions were administered during follow-up. However, at the 15-month follow-up, Patient 2 still exhibited low immunoglobulin levels. She developed recurrent pulmonary infections in month 2, which were treated with intravenous antibiotics. B cell aplasia is another major cause of immunocompromise in patients receiving CAR-T therapy. In our study, two patients achieved B cell recovery within 3 months, while the other two had persistent B cell aplasia lasting beyond 3 months (Fig. 3b), regardless of relapse or disease progression. Interestingly, Patient 2 had rapid recovery from B cell aplasia by month 2, yet her hypogammaglobulinemia persisted for over 15 months.

Following infusion, $CD8^+$ T cells in all patients consisted predominantly of effector and effector memory subsets. In most cases, the proportion of these subsets either increased or remained stable during extended follow-up (Fig. 3c), a trend not observed in $CD4^+$ T cells (Extended Data Fig. 4b). However, this phenotypic feature of bulk T cells showed no strong association with clinical response. Instead, as we previously reported, the phenotype of CAR^+ T cells correlated more closely with CAR-T expansion and efficacy[9]. We also observed a transient lymphocyte reduction in all patients within hours after ESO-T01 infusion, a phenomenon also noted with KLN-1010[11]. To explore the underlying mechanism, we collected serum samples at baseline, 6 h and 2 days after infusion for Luminex multiplex cytokine assay. Notably, most cytokines and chemokines, including those critical for T cell trafficking such as CXCL9, CXCL10 and CXCL11, increased by a 100- to a 1,000-fold shortly after infusion. This surge coincided with the sharp decline in lymphocyte counts. By day 2, cytokine levels typically decreased, with some returning to baseline, paralleling the onset of lymphocyte recovery in peripheral blood (Fig. 3d, Extended Data Fig. 4c and Supplementary Table 1). Therefore, we propose that chemokines released upon immune activation drove T cell migration.

Exploratory analyses of immunogenicity and genotoxicity associated with ESO-T01

Given the immunogenic potential of both the lentiviral vector and CAR construct, we also assessed the generation of antidrug antibodies. Using semi-quantitative kit, we found that Patients 1 and 2 had detectable anti-vesicular stomatitis virus glycoprotein (VSVG) antibodies at baseline, which slightly increased after infusion. Patient 3 exhibited no significant changes in antibody levels throughout the treatment course. In contrast, Patient 4 had an anti-VSVG antibody level at baseline below the threshold observed in samples from healthy donors (Fig. 4a). We suspect that this may be associated with the most pronounced immune activation and the highest cytokine release following infusion in Patient 4. As for anti-CAR antibodies, levels were relatively low in all but the first patient, who showed a slight elevation. To further explore this, we also evaluated immune thrombocytopenia (ITP) patients who received ex vivo BCMA-targeted CAR-T cells using the same CAR construct as ESO-T01, and observed similarly low levels of anti-CAR antibodies (Fig. 4b).

Another concern regarding the lentiviral vectors lies in the integration mutagenesis[13], which may lead to the transformation of T cells and even other somatic cells. In our patients, we did not observe meaningful secondary expansion of CAR-T cells after infusion (Fig. 2b). At the peak of expansion, integration sites were predominantly located on chromosome 17 (Extended Data Fig. 5a,b), similar to the previous findings in conventional ex vivo CAR-T cells[14]. The proportion of clones at integration sites associated with tumors or previously confirmed adverse events, did not exceed 3% in any case (Fig. 4c,d). In all patients, the top 10 clones accounted for less than 10% of the total, suggesting an absence of clonal expansion and a polyclonal pattern (Fig. 4e,f). Three months after infusion of ESO-T01, CAR-T cells remained at very low levels in the peripheral blood, and no high-risk integration events were detected. As expected, the genotoxicity of ESO-T01 was negligible.

Sensitivity analyses

Due to the small sample size and the early-phase study design, no formal sensitivity analyses were performed.

Post hoc analysis

After a protocol amendment, the subsequent three patients received prophylactic intravenous dexamethasone of 20 mg at 1 h before ESO-T01 infusion. This adjusted regimen did not impair CAR-T cell expansion and cause additional adverse events. Most adverse events resolved with standard clinical management. Notably, all patients exhibited early lymphocyte disappearance after infusion, and we measured cytokine and chemokine levels at baseline, 6 h and 2 days after infusion. We also analyzed the clinical outcomes of the three patients who received salvage therapies after disease progression. Salvage therapies prolonged their survival; however, treatment-related adverse events warrant attention. One patient received ex vivo BCMA-GPRC5D bispecific CAR-T cells after progression. The safety, efficacy and cellular kinetics of this subsequent treatment are described. These post hoc analyses are exploratory and hypothesis-generating, and our findings should be confirmed in prospective studies.

Discussion

To date, this report provides the long-term follow-up results for in vivo CAR-T therapy, with the longest follow-up reaching 15 months. All patients achieved an objective response and one patient maintained sCR for 15 months. However, three patients experienced early relapse or disease progression involving multiple extramedullary lesions and the CSF. Most of them had extensive extramedullary disease or CSF involvement and were relapsed or refractory at baseline, suggesting poor T cell fitness. Therefore, even with CAR-T cell expansion in the CSF, the local tumor burden may have overwhelmed the CAR-T cells. Furthermore, the inhibitory immune microenvironment and antigen downregulation may also play important roles. By contrast, Patient 2 had the lowest baseline tumor burden, with only two paraskeletal lesions, and did not receive corticosteroids at CAR-T expansion phase, which may have preserved CAR-T cell expansion and function. Notably, her CAR-T cells displayed a predominantly naive and central memory phenotype, and a second expansion of CAR-T cells was detected by qPCR at month 3, suggesting the persistence of a long-lived memory-like population. In addition, her younger age and fewer prior lines of therapy may have contributed to a more favorable T cell status, potentially enabling superior CAR-T cell fitness and persistence. While it is not possible to definitively attribute her sustained 15-month sCR to any single factor, these features collectively highlight the potential importance of host-related factors in determining long-term response durability.

The 'lymphocyte disappearance' observed within a few hours after infusion is relatively specific for in vivo CAR-T therapy, typically accompanied by a rapid onset of fever and chills[9–11]. Interestingly, counts of other blood cells, such as neutrophils and platelets, remain unchanged. Potential mechanisms underlying this phenomenon may

https://doi.org/10.1038/s41591-026-04704-z

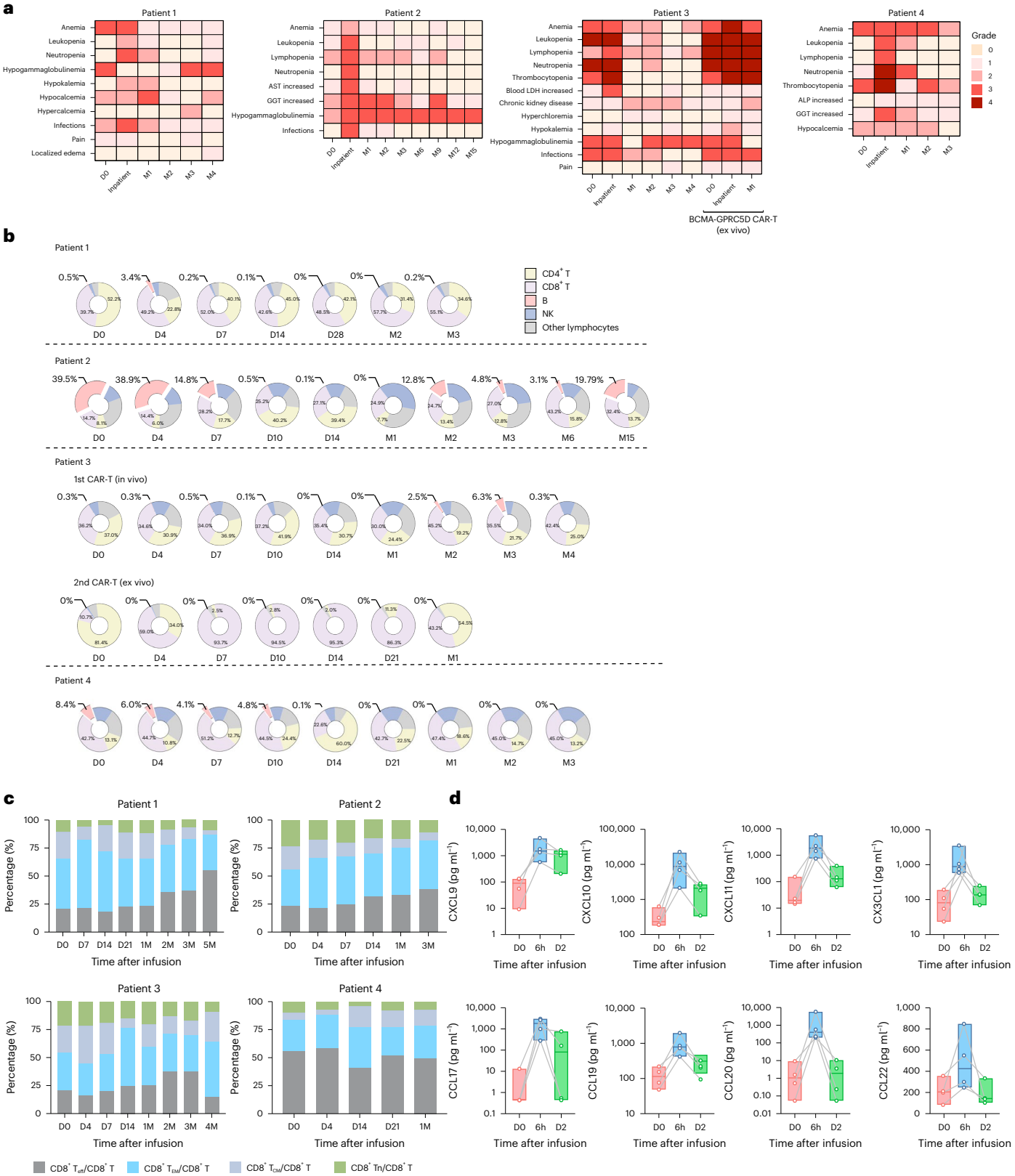


Fig. 3 | Adverse events and immune reconstitution following in vivo CAR-T treatment. a, The long-term adverse events associated with ESO-T01 during follow-up. Adverse events were graded according to the Common Terminology Criteria for Adverse Events (CTCAE) v5.0. **b**, Longitudinal distribution of peripheral lymphocyte subsets in patients 1–4 at different time points, illustrating B cell aplasia and recovery. **c**, Longitudinal profiling of $CD8^+$ T cell immunophenotypes in all patients by flow cytometry. **d**, Luminex proteomic analysis for serum concentrations of key T cell chemokines (for example, CXCL9, CXCL10, CXCL11, CX3CL1, CCL17, CCL19, CCL20 and CCL22) at baseline, 6 h and 2 days after infusion. Data are shown from four patients, and each data point represents one individual patient. No technical replicates were performed; each value is derived from a single measurement per patient sample. Data are presented as box plots where the horizontal line represents the median, and the bars extend from the minimum to the maximum values. T cells in Fig. 3b,c refer to pan-T cells instead of CAR^+ T cells. ALP, alkaline phosphatase; AST, aspartate aminotransferase; GGT, gamma-glutamyl transferase; LDH, lactate dehydrogenase; T_{eff}, effector T cell.

https://doi.org/10.1038/s41591-026-04704-z

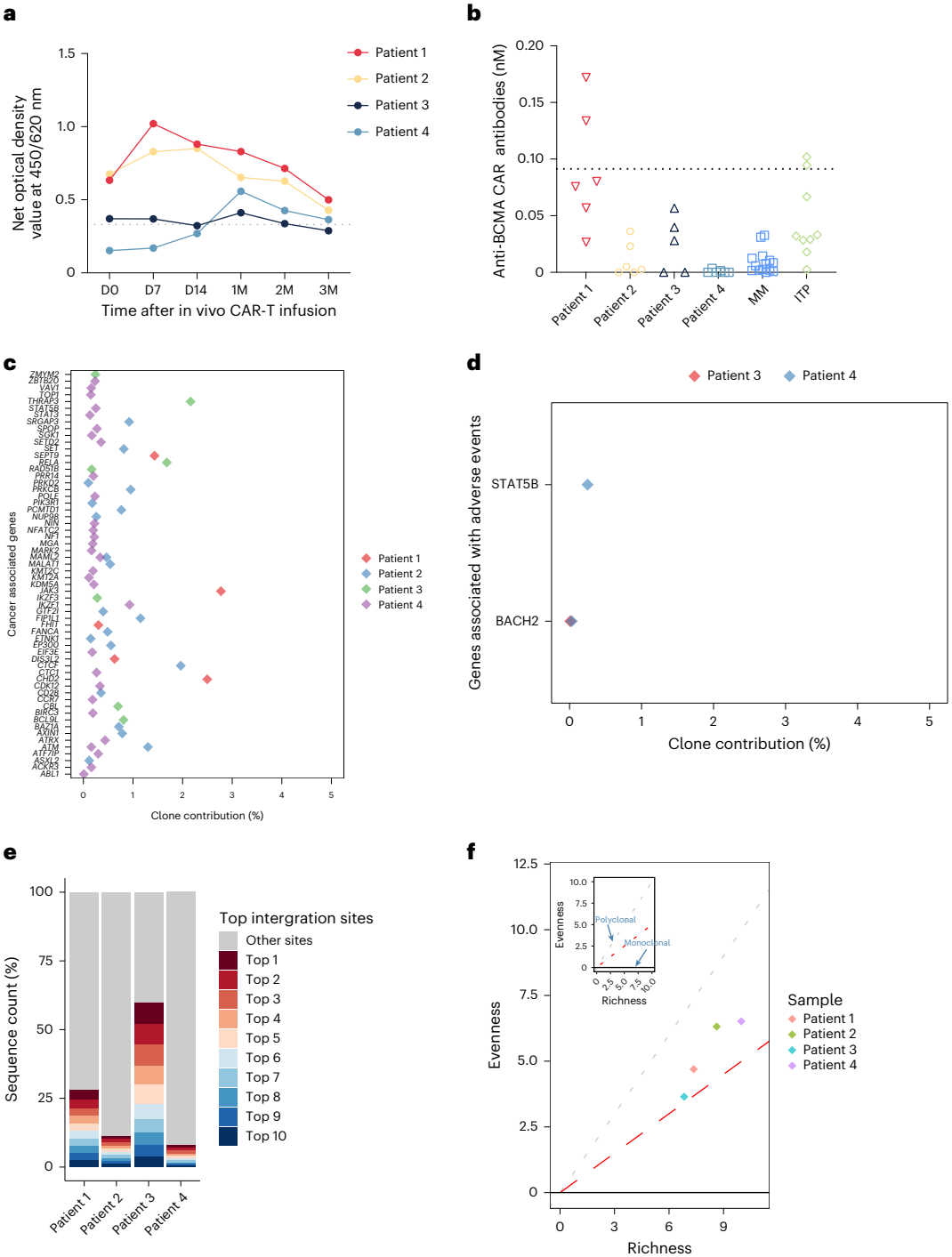


Fig. 4 | Immunogenicity and genotoxicity of in vivo CAR-T therapy. a, Plasma anti-VSVG antibody levels in all patients at indicated time points. The dashed line indicates the mean value of six healthy donors. **b**, Plasma anti-CAR antibody levels in all patients and controls. MM, patients with MM receiving ex vivo BCMA CAR-T with different anti-BCMA scFv; ITP, patients with ITP receiving ex vivo CAR-T with the same anti-BCMA VHH. The dashed line indicates the mean value of eight healthy donors. **c**, Integration sites located near tumor-associated genes. **d**, Integration sites located near genes previously associated with adverse events. **e**, Proportion of the top 10 integration clones in the samples. **f**, Polyclonality detection in samples from all patients. scFv, single-chain fragment variable; VHH, variable domain of heavy-chain antibodies.

include: (1) increased adhesion of lymphocytes to the vascular endothelium under lentiviral stimulation[15]; (2) activation of apoptotic pathways by the viral vectors[16], causing extensive programmed lymphocyte death; and (3) high viral loads in the bloodstream triggering immune activation and the release of cytokines and chemokines[17,18], which drive lymphocyte migration out of the circulation. Based on our measurements of a series of cytokines and chemokines, the last possibility is more likely, although other mechanisms cannot be completely ruled out. Furthermore, whether this phenomenon correlates with efficacy remains to be explored in a larger cohort.

Immune effector cell-associated hematotoxicity represents an important advantage of in vivo CAR-T over ex vivo CAR-T. For Ex vivo CAR-T therapy, lymphodepleting conditioning not only increases the risk of cytokine release syndrome, but also causes prolonged

hematologic toxicity after CAR-T infusion[19,20]. Moreover, some patients develop infections after lymphodepletion[21], which can delay or even preclude CAR-T infusion. In the KarMMA study, which also enrolled heavily pretreated patients, 41% and 48% of patients experienced prolonged grade 3 to 4 neutropenia and thrombocytopenia, respectively, lasting more than 1 month after treatment[22]. By contrast, owing to the absence of lymphodepleting chemotherapy and bridging therapy, patients treated with in vivo CAR-T generally recover more rapidly from hematologic toxicities.

Several studies have confirmed that early B cell recovery after CD19-targeted CAR-T therapy predicts CAR-T loss and disease relapse[23–25]. For BCMA-targeted CAR-T therapy, although the incidence of B cell aplasia can reach 100% (ref. 26), its correlation with clinical efficacy remains unestablished. Given BCMA is only expressed on mature B cells and plasma cells[27], BCMA CAR-T thus spares early $CD19^+$ B cells. Consequently, B cell recovery typically precedes plasma cell regeneration, which is consistent with our findings. In our study, the disease relapse or progression did not show strong correlation with B cell recovery, and the only patient with sustained sCR had B cell recovery within 2 months. In this patient, persistent hypogammaglobulinemia may be explained by the elimination of $CD19^-$, $BCMA^+$ long-lived plasma cells by BCMA-targeted CAR-T[19,28]. This highlights that patients remain at risk for infection long after CAR-T cell contraction and initial B cell compartment reconstitution, necessitating ongoing monitoring of immunoglobulin levels and supportive therapy with intravenous immunoglobulin infusions. An inverse correlation has been suggested between IgM recovery and progression-free survival[26]. However, none of our patients achieved IgM recovery during follow-up, precluding any analysis of this association. These issues warrant further exploration, particularly without lymphodepletion.

Lentiviral vectors are considered ideal vehicles for delivering transgenes due to their ability to carry large transgene cassettes, transduce both dividing and nondividing cells, and integrate the transgene into the host genome for stable expression[29]. Additionally, their lack of pre-existing antibodies and low anti-vector host immunity make them especially valuable[29]. As a result, lentiviral vectors are frequently utilized in vector-based vaccines. However, the immunogenicity of these vectors remains a key consideration in clinical applications[30]. In ex vivo CAR-T therapy, immunogenicity primarily arises from the heterogeneity of the antigen-binding domain[31]. In contrast, the immunogenicity of in vivo CAR-T therapy is influenced not only by the antigen-binding domain but also by the presence of anti-envelope immunity. Our observations indicate transient elevations in anti-VSVG IgG in some patients following infusion. However, despite having detectable baseline anti-VSVG antibodies, Patient 2 achieved the most durable response. Given that viral particles are cleared within 48 h after infusion, the clinical relevance of these antibodies remains elusive. Additionally, in the design of ESO-T01, the antigen-binding domain was selected from an anti-BCMA nanobody, which not only enhances the in vivo transduction efficiency of the vector, but also effectively reduces the production of anti-CAR antibodies.

The genotoxicity of lentiviral vectors has been a major concern in clinical applications due to their integrating nature. Fraietta et al.[32] reported that biallelic disruption of *TET2* (human TET2; NCBI Gene ID: 54790) via lentiviral integration drove massive CAR-T clonal expansion and an exceptional response in a patient with chronic lymphocytic leukemia. Extended analysis of integration sites in 39 additional patients revealed that insertional mutagenesis can modulate CAR-T proliferation and influence clinical outcomes, with certain integration events (such as those involving *TET2* and *TGFBR2* (human TGFBR2, NCBI Gene ID: 7048)) correlating with superior efficacy[33]. Similarly, in a patient with acute lymphoblastic leukemia treated with anti-CD22 CAR-T, delayed re-expansion of CAR-T cells harboring *CBL* (human CBL, NCBI Gene ID: 867) integration led to complete regression of residual extramedullary disease[34]. However, insertional mutagenesis does not always play a positive role. It can also drive malignant transformation. For example, random integration of CAR transgene into the *TP53* (human TP53, NCBI Gene ID: 7157) locus of a $CD4^+$ T cell led to the development of T cell lymphoma involving the digestive tract[35]. Harrison et al.[36] also described a CAR^+ tumor linked to pre-existing somatic variants in *NFKB2* (human NFKB2, NCBI Gene ID: 4791), *TET2, JAK 3* (human JAK3, NCBI Gene ID: 3718) *or PTPRB* (human PTPRB, NCBI Gene ID: 5787), while Ozdemirli et al.[37] documented a secondary T cell lymphoma with a single lentiviral insertion in intron 2 of *SSU72*. Although no high-risk insertional mutagenesis events were observed in our small-scale study at the expansion peak and 3 months after infusion, larger cohort and longer follow-up is warranted to explore the possibility.

We also explored the feasibility of administering diversified treatments following in vivo CAR-T therapy. Among patients receiving chemotherapy as salvage therapy, one patient attained sCR and one remained stable disease, with overall survival prolonged to 8 and 11 months, respectively, in these heavily pretreated patients. More importantly, one patient who progressed after in vivo CAR-T subsequently received ex vivo CAR-T therapy and achieved a VGPR. The successful infusion and robust expansion of ex vivo CAR-T cells of this patient suggest that prior in vivo CAR-T therapy does not interfere with the collection, manufacturing or proliferation of subsequent conventional CAR-T cells, and may instead offer some patients an opportunity for subsequent ex vivo CAR-T therapy. However, antigen escape remains a pivotal limitation. Though BCMA loss is rarely reported and is usually associated with pre-existing or emerging gene mutations at TNFRSF17 locus[38,39]. In our study, the extramedullary and medullary biopsies demonstrated BCMA-dim and -negative expression in Patient 3, which necessitated the use of bispecific CAR-T therapy. For the remaining two patients, BCMA expression status remained unknown: extramedullary lesion specimens were unavailable, and our institutional standard diagnostic panels for MRD in the CSF did not routinely include BCMA staining. Future prospective studies should therefore mandate BCMA expression profiling at relapse to clarify the role of antigen escape in treatment resistance.

The major limitations included the small sample size, an incomplete mechanistic understanding of both early lymphocyte disappearance and relapse of extramedullary disease. Larger cohort studies with extended follow-up are therefore warranted. Furthermore, many of our analyses were post hoc, and these findings need to be validated in prospective studies. Nonetheless, these results may inform the design of future research.

In summary, our study establishes the feasibility and safety of in vivo CAR-T therapy in multiple myeloma, extending the proof of concept to hematologic malignancies. Moving forward, efforts should be focused on improving the durability of remission—a critical goal that will shape the next generation of innovation in this field.

Online content

Any methods, additional references, Nature Portfolio reporting summaries, source data, extended data, supplementary information, acknowledgements, peer review information; details of author contributions and competing interests; and statements of data and code availability are available at https://doi.org/10.1038/s41591-026-04704-z.

References

1. Longo, D. L. Engineering CAR T cells for off-the-shelf use. *N. Engl. J. Med.* **389**, 953–957 (2023).
2. Al Hadidi, S. et al. Clinical outcome of patients with relapsed refractory multiple myeloma listed for BCMA directed commercial CAR-T therapy. *Bone Marrow Transplant.* **58**, 443–445 (2022).
3. Bot, A. et al. In vivo chimeric antigen receptor (CAR)-T cell therapy. *Nat. Rev. Drug Discov.* **25**, 116–137 (2025).
4. Xu, J., Chen, Z., Su, L., Ren, A. & Mei, H. In vivo CAR cell therapy: from bench to bedside. *J. Hematol. Oncol.* **18**, 105 (2025).

5. Nicolai, C. J. et al. In vivo CAR T-cell generation in nonhuman primates using lentiviral vectors displaying a multidomain fusion ligand. *Blood* **144**, 977–987 (2024).
6. Andorko, J. I. et al. Targeted in vivo delivery of genetic medicines utilizing an engineered lentiviral vector platform results in CAR T and NK cell generation. *Mol. Ther.* **33**, 4937–4952 (2025).
7. Hunter, T. L. et al. In vivo CAR T cell generation to treat cancer and autoimmune disease. *Science* **388**, 1311–1317 (2025).
8. Lemgart, V. T. et al. Reprogramming CD22 CAR-T cells in vivo using CD8-targeted mRNA-LNPs to treat hematological malignancies. *Mol. Ther.* **34**, 2621–2636 (2026).
9. Xu, J. et al. In-vivo B-cell maturation antigen CAR T-cell therapy for relapsed or refractory multiple myeloma. *Lancet* **406**, 228–231 (2025).
10. Wang, Q. et al. In vivo CD19 CAR T-cell therapy for refractory systemic lupus erythematosus. *N. Engl. J. Med.* **393**, 1542–1544 (2025).
11. Harrison, S. et al. Minimal residual disease (MRD)-negative outcomes following a novel, in vivo gene therapy generating anti-B-cell maturation antigen (BCMA) chimeric antigen receptor (CAR)-T cells in patients with relapsed and refractory multiple myeloma (RRMM): preliminary results from inMMyCAR, the first-in-human phase 1 study of KLN-1010. *Blood* **146**, LBA-1 (2025).
12. Yan, W. et al. Uncommon biphasic CAR-T expansion induces hemophagocytic lymphohistiocytosis-like syndrome and fatal multiple infections following BCMA CAR-T cell therapy: a case report. *J. Immunother. Cancer* **12**, e010080 (2024).
13. Jadlowsky, J. K. et al. Long-term safety of lentiviral or gammaretroviral gene-modified T cell therapies. *Nat. Med.* **31**, 1134–1144 (2025).
14. Gabriel, R. et al. Comprehensive genomic access to vector integration in clinical gene therapy. *Nat. Med.* **15**, 1431–1436 (2009).
15. Reyat, J. S., Tomlinson, M. G. & Noy, P. J. Utilizing lentiviral gene transfer in primary endothelial cells to assess lymphocyte-endothelial interactions. *Methods Mol. Biol.* **1591**, 155–168 (2017).
16. Abiri, E., Mirzaii, M., Moghbeli, M., Atashi, A. & Harati, A. A. Investigating the relationship between lymphocyte cells apoptosis and DNA damage and oxidative stress and therapeutic and clinical outcomes of COVID-19 elderly patients. *BMC Infect. Dis.* **24**, 940 (2024).
17. Cousin, C. et al. Persistence of integrase-deficient lentiviral vectors correlates with the induction of STING-independent $CD8^+$ T cell responses. *Cell Rep.* **26**, 1242–1257.e7 (2019).
18. Breckpot, K. et al. Activation of immature monocyte-derived dendritic cells after transduction with high doses of lentiviral vectors. *Hum. Gene Ther.* **18**, 536–546 (2007).
19. Brudno, J. N. & Kochenderfer, J. N. Current understanding and management of CAR T cell-associated toxicities. *Nat. Rev. Clin. Oncol.* **21**, 501–521 (2024).
20. Amini, L. et al. Preparing for CAR T cell therapy: patient selection, bridging therapies and lymphodepletion. *Nat. Rev. Clin. Oncol.* **19**, 342–355 (2022).
21. Mikkilineni, L. et al. Infectious complications of CAR T-cell therapy across novel antigen targets in the first 30 days. *Blood Adv.* **5**, 5312–5322 (2021).
22. Munshi, N. C. et al. Idecabtagene vicleucel in relapsed and refractory multiple myeloma. *N. Engl. J. Med.* **384**, 705–716 (2021).
23. Hill, J. A. et al. Durable preservation of antiviral antibodies after CD19-directed chimeric antigen receptor T-cell immunotherapy. *Blood Adv.* **3**, 3590–3601 (2019).
24. Song, F. et al. Safety and efficacy of autologous and allogeneic humanized CD19-targeted CAR-T cell therapy for patients with relapsed/refractory B-ALL. *J. Immunother. Cancer* **11**, e005701 (2023).
25. Yin, Z., Zhang, Q., Zhu, Y. & Liu, S. From response to cure: unaddressed clinical challenges in the Tali-cel™ CD19 CAR-T trial for relapsed/refractory pediatric B-cell acute lymphoblastic leukemia. *Blood Cancer J.* **15**, 180 (2025).
26. Wang, Y. et al. Humoral immune reconstitution after anti-BCMA CAR T-cell therapy in relapsed/refractory multiple myeloma. *Blood Adv.* **5**, 5290–5299 (2021).
27. Shah, N., Chari, A., Scott, E., Mezzi, K. & Usmani, S. Z. B-cell maturation antigen (BCMA) in multiple myeloma: rationale for targeting and current therapeutic approaches. *Leukemia* **34**, 985–1005 (2020).
28. O'Connor, B. P. et al. BCMA is essential for the survival of long-lived bone marrow plasma cells. *J. Exp. Med.* **199**, 91–98 (2004).
29. Hu, B., Tai, A. & Wang, P. Immunization delivered by lentiviral vectors for cancer and infectious diseases. *Immunol. Rev.* **239**, 45–61 (2011).
30. Annoni, A., Gregori, S., Naldini, L. & Cantore, A. Modulation of immune responses in lentiviral vector-mediated gene transfer. *Cell Immunol.* **342**, 103802 (2018).
31. Wagner, D. L. et al. Immunogenicity of CAR T cells in cancer therapy. *Nat. Rev. Clin. Oncol.* **18**, 379–393 (2021).
32. Fraietta, J. A. et al. Disruption of TET2 promotes the therapeutic efficacy of CD19-targeted T cells. *Nature* **558**, 307–312 (2018).
33. Nobles, C. L. et al. CD19-targeting CAR T cell immunotherapy outcomes correlate with genomic modification by vector integration. *J. Clin. Invest.* **130**, 673–685 (2020).
34. Shah, N. N. et al. Clonal expansion of CAR T cells harboring lentivector integration in the CBL gene following anti-CD22 CAR T-cell therapy. *Blood Adv.* **3**, 2317–2322 (2019).
35. Perica, K. et al. $CD4^+$ T-cell lymphoma harboring a chimeric antigen receptor integration in TP53. *N. Engl. J. Med.* **392**, 577–583 (2025).
36. Harrison, S. J. et al. CAR+ T-cell lymphoma after cilta-cel therapy for relapsed or refractory myeloma. *N. Engl. J. Med.* **392**, 677–685 (2025).
37. Ozdemirli, M. et al. Indolent $CD4^+$ CAR T-cell lymphoma after cilta-cel CAR T-cell therapy. *N. Engl. J. Med.* **390**, 2074–2082 (2024).
38. Lee, H. et al. Mechanisms of antigen escape from BCMA- or GPRC5D-targeted immunotherapies in multiple myeloma. *Nat. Med.* **29**, 2295–2306 (2023).
39. Samur, M. K. et al. Biallelic loss of BCMA as a resistance mechanism to CAR T cell therapy in a patient with multiple myeloma. *Nat. Commun.* **12**, 868 (2021).

Publisher's note Springer Nature remains neutral with regard to jurisdictional claims in published maps and institutional affiliations.

Open Access This article is licensed under a Creative Commons Attribution-NonCommercial-NoDerivatives 4.0 International License, which permits any non-commercial use, sharing, distribution and reproduction in any medium or format, as long as you give appropriate credit to the original author(s) and the source, provide a link to the Creative Commons licence, and indicate if you modified the licensed material. You do not have permission under this licence to share adapted material derived from this article or parts of it. The images or other third party material in this article are included in the article's Creative Commons licence, unless indicated otherwise in a credit line to the material. If material is not included in the article's Creative Commons licence and your intended use is not permitted by statutory regulation or exceeds the permitted use, you will need to obtain permission directly from the copyright holder. To view a copy of this licence, visit http://creativecommons.org/licenses/by-nc-nd/4.0/.

© The Author(s) 2026

https://doi.org/10.1038/s41591-026-04704-z

Jia Xu[1,2,3,4], Lin Liu[1,2,3,4], Wei Xie[1,2,3,4], Liman Su[1,2,3,4], Weijiayi Wang[1,2,3], Chenggong Li[1,2,3], Qiaolin Liu[1,2,3], Yun Kang[1,2,3], Yinqiang Zhang[1,2,3], Wenjing Luo[1,2,3], Zhongpei Huang[1,2,3], Chun Zhang[1,2,3], Chunyan Sun[1,2,3], Yu Hu[1,2,3] ✉ & Heng Mei[1,2,3] ✉

[1]Institute of Hematology, Union Hospital, Tongji Medical College, Huazhong University of Science and Technology, Wuhan, China. [2]Hubei Clinical Medical Center of Cell Therapy for Neoplastic Disease, Wuhan, China. [3]Key Laboratory of Biological Targeted Therapy (Huazhong University of Science and Technology), The Ministry of Education, Wuhan, China. [4]These authors contributed equally: Jia Xu, Lin Liu, Wei Xie, Liman Su. ✉e-mail: dr_huyu@126.com; hmei@hust.edu.cn

Methods

Clinical study design

This phase 1, single-arm, open-label study was conducted at Wuhan Union Hospital, Huazhong University of Science and Technology, China. The aim was to evaluate the safety, tolerability and preliminary efficacy of ESO-T01, a third-generation, non-replicating, self-inactivating lentiviral vector encoding anti-BCMA CAR, in patients with R/R MM. This study was approved by the Ethics Committee of the Union Hospital affiliated to Huazhong University of Science and Technology, Wuhan, China (REC ref no. (2024) 0915-02). The study was registered in ClinicalTrials.gov (NCT06691685) on 9 November 2024. Due to the acquisition of the sponsor, EsoBiotec, by AstraZeneca, the study was terminated, and no more patients were enrolled.

The protocol was amended once to allow prophylactic use of glucocorticoid before infusion, to include patients who suffered from clinical relapse (including new bone lesions or confirmed increase (≥50% increase in sum of the products of the diameters of measurable lesions with an absolute value of ≥1 cm) of lesions or soft-tissue plasmacytomas), to specify that urine protein electrophoresis, urine immunofixation electrophoresis, and urine free light chain assessments are performed on 24-h urine collections; and to accept test results obtained within 7 days before screening as valid screening data. The protocol accompanying our previously published report[9] was the amended version.

All participants provided written informed consent before any study-related procedures. Participants received study treatment and related procedures free of charge. Reimbursement for transportation and nutrition was provided for each blood collection and follow-up visit.

Sex was assessed via participant self-report. Due to the small size of the cohort, neither sex nor gender was considered in the enrollment criteria and disaggregated analysis by sex was not performed.

Inclusion criteria

Major inclusion criteria were as follows: age ≥ 18 years, any sex; confirmed diagnosis of MM according to the International Myeloma Working Group criteria with positive BCMA expression on MM cells confirmed by flow cytometry or bone marrow pathology and immunohistochemistry; at least two prior lines of therapy; relapse or disease progression within 12 months before screening; refractoriness to both immunomodulators and proteasome inhibitors; PD during or within 2 months after the most recent antimyeloma therapy; measurable disease as defined as follows; an Eastern Cooperative Oncology Group performance status score of 0–2 and an expected survival of ≥3 months. Measurable disease was defined as serum M protein ≥0.5 g dl^{-1}, or urine M protein ≥200 mg per 24 h, or involved serum free light chain ≥10 mg dl^{-1} with an abnormal free light chain κ/λ ratio, or clinical relapse (new bone lesions or soft tissue plasmacytomas, excluding osteoporotic fractures, or a confirmed increase of ≥50% in the sum of the products of diameters of measurable lesions, with an absolute value of ≥1 cm, in pre-existing plasmacytomas or bone lesions).

In addition, patients were required to meet the following criteria at screening or within 2 months before screening: bone marrow function tests showing hemoglobin ≥6 g dl^{-1} (red blood cell transfusions permitted to maintain this level, and erythropoietin allowed), absolute neutrophil count ≥600 μl^{-1} (without G-CSF within 1 week or pegylated G-CSF within 2 weeks before screening), platelet count ≥50,000 μl^{-1}, lymphocyte count ≥500 μl^{-1}, and absolute $CD3^+$ T cell count ≥150 μl^{-1}; renal function with creatinine clearance ≥45 ml min^{-1} (Cockcroft–Gault formula); liver function with ALT/AST ≤3.0 × ULN, total bilirubin and ALP ≤2.0 × ULN (except congenital hyperbilirubinemia such as Gilbert's syndrome, where direct bilirubin ≤1.5 × ULN), and albumin ≥3 g dl^{-1}; cardiac function with left ventricular ejection fraction ≥40%, no clinically important pericardial effusion or electrocardiogram abnormalities; pulmonary function with oxygen saturation ≥90% and no clinically important pleural effusion. Women of childbearing potential must have a negative pregnancy test at screening and before infusion and must not be breastfeeding. Both men and women of childbearing potential must agree to use effective contraception and not to donate germ cells (sperm or oocytes) from the time of signing informed consent until one year after study drug administration. Finally, the subject or a legally authorized representative must provide written informed consent.

Exclusion criteria

Exclusions related to prior treatment comprised: targeted, epigenetic or investigational therapies within 5 half-lives; systemic or cytotoxic therapy within 1 week; proteasome inhibitors or immunomodulators within 2 weeks; radiotherapy within 4 weeks (except when ≤5% of bone marrow reserve was irradiated); allogeneic hematopoietic stem cell transplantation within 6 months or autologous hematopoietic stem cell transplantation within 3 months; prior treatment with a VSVG-pseudotyped virus; and live-attenuated vaccines within 1 month. Disease-related exclusions included active second malignancies (nonmelanoma skin cancer excepted), uncontrolled serious infections, and positive serology for HBV, HCV, HIV or syphilis. Organ dysfunction exclusions were severe heart failure (NYHA class III or IV), myocardial infarction or revascularization within 6 months, clinically important arrhythmias and severe cardiomyopathy. Other exclusions comprised primary immunodeficiency, stroke or seizure within 6 months, dementia, Parkinson's disease, surgery within 2 weeks, severe allergies to ESO-T01 or tocilizumab, lack of venous access and investigator discretion.

Study endpoints and assessment

The primary endpoints were the safety and tolerability of ESO-T01. Safety parameters included dose-limiting toxicities, adverse events, laboratory tests, vital signs, physical examinations and electrocardiograms. The secondary endpoints were efficacy, pharmacokinetics and pharmacodynamics. Efficacy parameters included time to response, objective response rate, MRD negativity rate, duration of response, progression-free survival, overall survival, objective response rate included sCR, complete response, VGPR and PR. Pharmacokinetic parameters included maximum concentration, time to maximum concentration and area under the curve from time 0 to day 28, for the expansion of BCMA CAR-T cells in peripheral blood after ESO-T01 infusion. Pharmacodynamic parameters included testing of cytokine levels (for example, IL-6, IL-10, IFNγ and TNF), C-reactive protein, ferritin levels, immunoglobulin levels (IgG, IgA, IgM and IgE) and peripheral lymphocyte subpopulations (T, B, NK cell ratios and absolute counts) in peripheral blood after ESO-T01 infusion. The exploratory endpoint was the immunogenicity of ESO-T01 and in vivo generated CAR-T cells by ESO-T01, as well as the presence of shedding of ESO-T01 in blood, saliva, urine and feces. This report focuses on updated safety and efficacy outcomes. The endpoints including safety and tolerability along with early-phase pharmacokinetics or pharmacodynamics profiles have been reported previously in our initial publication on this cohort, and are therefore summarized briefly rather than presented in full here.

Toxicities occurring within 28 days after infusion were recorded as dose-limiting toxicities and graded according to CTCAE v5.0, while CRS and ICANS were graded per the American Society for Transplantation and Cellular Therapy consensus criteria. Beyond 28 days, laboratory abnormalities and other adverse events collected during follow-up visits continued to be graded using CTCAE v5.0. Efficacy evaluation was based on 2016 IMWG criteria.

Lentiviral vector and CAR construct design and production

The CAR backbone of ESO-T01 (PRG1801, WO2025/003526A1 and CN109134665B) consists of an anti-BCMA nanobody (VHH), a CD8α hinge and transmembrane domain, a 4-1BB co-stimulatory domain and a CD3ζ signaling domain, all under the control of a synthetic T cell-specific promoter. To enhance T cell selectivity and reduce

off-target transduction, ESO-T01 incorporates additional modifications, including a mutant VSVG envelope, CD47 overexpression, MHC-I knockout and an anti-TCR nanobody. Further details of the vector design, its underlying mechanisms and the Good Manufacturing Practice manufacturing process have been described previously in our earlier report[9] and in the study by An et al.[40].

Monitoring of CAR-T cells

Surface expression of CAR-transduced T cells in CSF was determined by flow cytometry at the sensitivity of 10^{-5}. Precision count beads (424902; Biolegend) were used for quantification. CSF (1 ml) was incubated with 10 µl counting beads, centrifuged and washed once with PBS. Cells were then incubated with biotinylated human BCMA protein (BC7-H82F0; Acro) for 40 min, washed with PBS, and stained with CD3 APC (317317; Biolegend) and PE-streptavidin (405204; Biolegend) for 15 min. After a final PBS wash, samples were resuspended for flow cytometry analysis. The qPCR was used to detect the vector copy number in four patients as we previously reported[9]. To better compare the expansion characteristics, CAR copies of in vivo BCMA CAR-T and ex vivo BCMA-GPRC5D CAR-T were detected using ddPCR. Genomic DNA from patient peripheral blood samples was extracted by TIANGEN Genomic DNA Extraction Kit DP340 and 40 ng DNA was used for one test. We used two sets of primers and probes. The first set targets the region spanning 4-1BB and CD3ζ, which is applicable to both in vivo and ex vivo CAR-T products in our study, allowing a better comparison of their differences in CAR-T kinetics. The forward primer was AGAGGAAGATGGCTGTAG; the reverse primer was CTGCTGAACTTCACTCTC; and the probe sequence was FAM-CACATCCTCCTTCTTCTTCTTCTGG-TAMRA (Tsinke, China). The second set targets the anti-BCMA VHH region of the in vivo CAR sequence, enabling specific detection of the kinetics of in vivo CAR-T cells. The forward primer was GGAATCGCTGACGGGTCAGA; the reverse primer was GGCTTCGCTGGGGAACTCA; and the probe sequence was FAM- CTTTGGCTCCTATGGACAGG-TAMRA (General Biol, China). The Bio-Rad CFX96 System was used for quantification.

Immunohistochemistry

Staining for CD38, CD138, CS1 and BCMA was performed on FFPE sections using a Titan automated stainer (Maixin Biotech). Following heat-induced epitope retrieval, sections were processed with a polymer-based detection system and DAB chromogen. Stained slides were digitized and quantified using QuPath v.0.4.3. The catalog of antibodies used for immunohistochemistry are provided in Supplementary Table 2.

Laboratory measurements

Levels of serum creatine kinase, hemoglobin, leukocyte, neutrophil, lymphocyte, platelet, AST, GGT, ferritin, K^+, Cl^-, Ca^{2+} and immunoglobins were measured in routine laboratory. Flow cytometry was used to analyze the proportion $CD4^+$ T cells, $CD8^+$ T cells, NK cells and B cells within lymphocytes, as well as T_n, T_{eff}, T_{CM} and T_{EM} subsets within $CD4^+$ and $CD8^+$ T cell subpopulations.

T cell phenotype detection

T cell phenotypes were analyzed by flow cytometry. Samples from peripheral blood were stained with the standardized panel: biotinylated human BCMA protein, Fixable Viability Stain 780 (BD, USA), CD3-Percp5.5, CD4-FITC, CD8-PE-Cy7, CD45RA-APC, CD62L-BV510, CD28-BV510, and CD57-PE594, PE-streptavidin. Stained samples were detected using BD FACSymphony A1 (BD) and analyzed using FlowJo software (TreeStar). The clone and catalog of these antibodies are provided in Supplementary Table 3.

Luminex assay

Serum samples were collected at indicated time points and stored at −80 °C until use. The serum of Patient 4 was diluted at a ratio of 1:3, while the serum of the other patients was diluted at a ratio of 1:2. Cytokine levels were measured using a BioPlex Pro Human Cytokine Screening 48-Plex Kit according to the manufacturer's instructions. Samples were processed on a Luminex 200 instrument, with data acquisition performed by Univ-Bio.

Measurement of vesicular stomatitis virus glycoprotein and CAR antibodies

Anti-VSVG antibodies were detected by ELISA kit (AE-327310-1; Alpha Diagnostic International) according to the manufacturer's instructions. Plasma samples from healthy donors and patients before and after infusion were collected. The absorbance (optical density value) was measured using Tecan Infinite F50 Microplate Reader. All samples were tested in duplicate wells. To detect anti-CAR antibodies, plasma samples were collected from patients receiving in vivo CAR-T (anti-BCMA VHH), as well as from control groups, including healthy donors, patients with MM receiving ex vivo CAR-T (different anti-BCMA scFv) and patients with ITP receiving ex vivo CAR-T (identical anti-BCMA VHH). For patients with MM, samples were obtained at baseline and after infusion; for patients with ITP, all samples were collected after infusion. Serially diluted BCMA-Fc protein was used as standards. CHO cells expressing BCMA CAR (lentivirus provided by Shenzhen Pregene Biopharma Co., Ltd) were incubated with plasma samples at 4 °C for 40 min, followed by PBS washes and stained with PE anti-human IgG Fc antibody. Serum antibodies concentrations were determined using a standard curve generated by plotting ΔMFI against the log molar concentration of the standards.

Integration site analysis

Lentiviral integration sites were mapped using standardized shearing extension primer tag selection ligation-mediated PCR (S-EPTS/LM-PCR) and next-generation sequencing. Genomic DNA was sheared and amplified with biotinylated primers specific to the viral long terminal repeat. Biotinylated fragments were captured on beads, ligated to barcoded linker, and enriched by nested PCR to incorporate sequencing-specific adapters and secondary barcodes. Final libraries were quantified by Qubit 4.0 and TapeStation 4150, and then sequenced on the MiSeq platform (Illumina)[14,41]. Data were processed using the Genome Integration Site Analysis pipeline (GENE-IS)[42] and R studio (LISA package)[43].

Statistical analysis

Data were derived from four patients treated with in vivo CAR-T and control groups (healthy donors, patients with MM treated with ex vivo BCMA CAR-T, and patients with ITP treated with ex vivo BCMA CAR-T). All statistical analyses were performed according to the guideline in section 9 of the study protocol. Sample sizes are as follows: Fig. 2a,b: $n = 4$ patients; Fig. 2c–f: $n = 1$ patient (Patient 3, female, 67 years); Fig. 3a–d: $n = 4$ patients; Fig. 4a: $n = 4$ patients (in vivo CAR-T) and $n = 6$ healthy donors; Fig. 4b: $n = 4$ patients receiving in vivo CAR-T (Day 0 and after infusion), $n = 5$ patients with MM receiving ex vivo BCMA CAR-T with different anti-BCMA scFv (Day 0 and after infusion), $n = 4$ patients with ITP treated with CAR-T using the identical anti-BCMA VHH (after infusion) and $n = 8$ healthy donors; Fig. 4c–f: $n = 4$ patients; Extended Data Fig. 1a: $n = 4$ patients: Extended Data Fig. 1b: $n = 1$ patient (Patient 3, female, 67 years): Extended Data Fig. 2: $n = 1$ patient (Patient 4, male, 59 years); Extended Data Fig. 3a: $n = 1$ patient (Patient 1, male, 69 years); Extended Data Fig. 3b: $n = 1$ patient (Patient 2, female, 40 years); Extended Data Fig. 3c–e: $n = 1$ patient (Patient 3, female, 67 years); Extended Data Fig. 3f: $n = 1$ patient (Patient 4, male, 59 years); Extended Data Fig. 4a–c: $n = 4$ patients; Extended Data Fig. 5a,b: $n = 4$ patients.

Because of the limited sample size ($n = 4$), we did not perform formal hypothesis testing, power calculation or inferential statistics. The sample size was not statistically predetermined, no data were excluded and the study was not randomized. The investigators were

not blinded to allocation during experiments and outcome assessment. Accordingly, all findings are presented descriptively. Data were analyzed using FlowJo v.10.6.1, GraphPad Prism v.10.4.1 and QuPath v.0.4.3. Additionally, to support reproducibility, the complete raw data and fully annotated analysis templates are available from the corresponding author upon reasonable request, under a standard data transfer agreement to protect participant privacy.

Reporting summary

Further information on research design is available in the Nature Portfolio Reporting Summary linked to this article.

Data availability

The summary data are included in this article and its Supplementary Information, which provides patient-level details on safety, response, pharmacokinetics, immunophenotyping, vector constructs, integration sites and gating strategies. Individual-level clinical datasets are not publicly available for proprietary and privacy reasons but have been de-identified and stored securely at Wuhan Union Hospital. Access may be granted to qualified researchers upon request to the corresponding author. Applicants must sign a data-use agreement defining the research scope, and commercial use is prohibited. After approvals from both the applicant's institution and our internal data access committee, de-identified data will be delivered within 6 months of request approval. Requests should be sent to hmei@hust.edu.cn. Responses will be given within 10 working days. The full trial protocol and statistical analysis plan are provided in the supplementary materials. Integration site sequencing data have been deposited in the Genome Sequence Archive for Human (GSA-Human) at the China National Center for Bioinformation (CNCB; https://ngdc.cncb.ac.cn/gsa-human/) under accession number HRA021285. Due to Chinese regulations on the administration of human genetic resources, these data are held under controlled access. De-identified individual-level sequencing data are available to qualified researchers for non-commercial academic use through the GSA-Human Data Access Request system.

References

40. An, N. et al. In vivo generation of anti-BCMA CAR-T cells in relapsed or refractory multiple myeloma: a phase 1 study. *Nat. Med.* **32**, 1257–1266 (2026).
41. Paruzynski, A. et al. Genome-wide high-throughput integrome analyses by nrLAM-PCR and next-generation sequencing. *Nat. Protoc.* **5**, 1379–1395 (2010).
42. Afzal, S., Wilkening, S., von Kalle, C., Schmidt, M. & Fronza, R. GENE-IS: time-efficient and accurate analysis of viral integration events in large-scale gene therapy data. *Mol. Ther. Nucleic Acids* **6**, 133–139 (2016).
43. Ni, S. et al. LISA: a comprehensive R package for lentiviral integration site analysis in gene therapy safety assessment. Preprint at *bioRxiv* https://doi.org/10.64898/2025.12.20.695672 (2025).

Acknowledgements

We thank the patients and their relatives, who gave consent for the study. We also appreciate Shanghai Waker Biotechnology Co., Ltd for providing professional technical support in the detection and analysis of integration sites in this study.

Author contributions

J.X., L.L. and H.M. contributed to paper writing and statistical analysis. H.M. and Y.H. conceptualized and supervised the study. J.X., L.L., W.X. and L.S. collected and analyzed the data. J.X., W.W., C.L., Q.L., Y.K., Y.Z., W.L. and Z.H. completed the related experiments and figure visualization. H.M., Y.H., C.S. and C.Z. took part in the revision of the manuscript.

Funding

This study was supported by the National Natural Science Foundation of China (nos. 82350103, 82425003 and 82330005), the National Science and Technology Major Project (no. 2026ZD1806000) and Shenzhen Pregene Biopharma, which supported patient follow-up, laboratory tests and technical input. The funders had no role in study design, data collection and analysis, decision to publish or preparation of the manuscript.

Competing interests

The authors declare no competing interests.

Additional information

Extended data is available for this paper at https://doi.org/10.1038/s41591-026-04704-z.

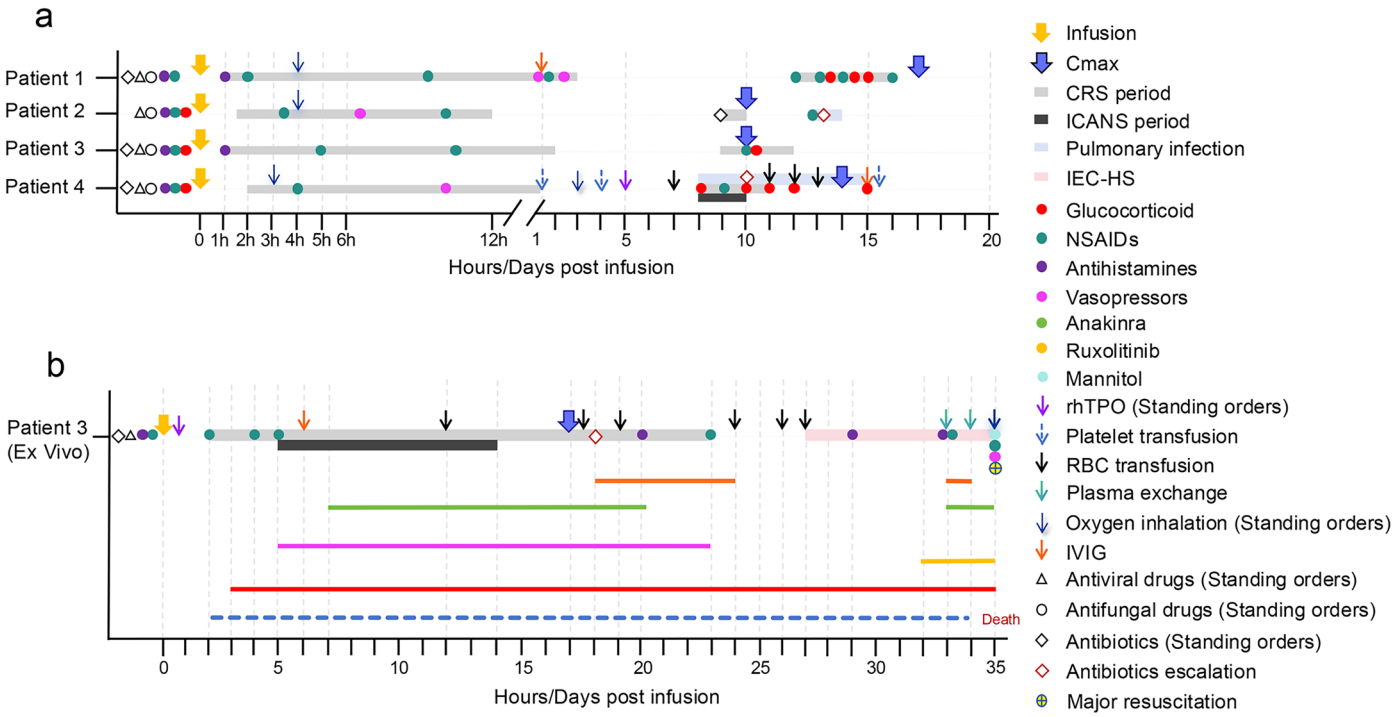
Supplementary information The online version contains supplementary material available at https://doi.org/10.1038/s41591-026-04704-z.

Correspondence and requests for materials should be addressed to Yu Hu or Heng Mei.

Peer review information *Nature Medicine* thanks Samir Parekh, Jae Park and Nathan Singh for their contribution to the peer review of this work. Peer reviewer reports are available. Primary Handling Editors: Anna Ranzoni and Saheli Sadanand, in collaboration with the *Nature Medicine* team.

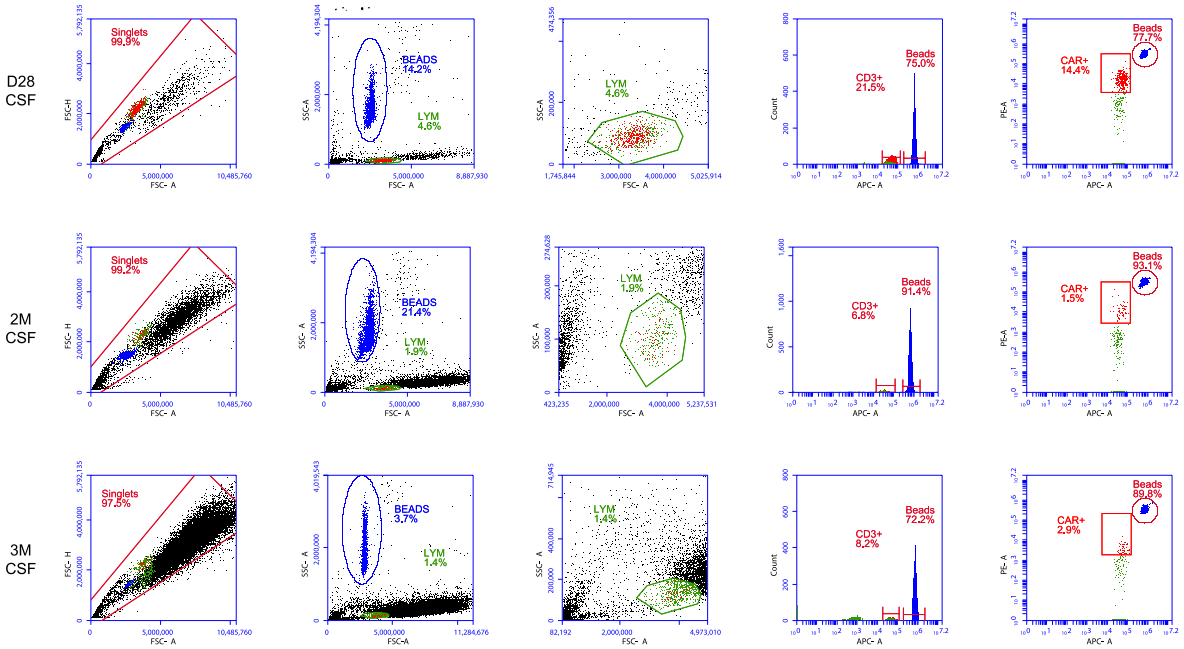
Reprints and permissions information is available at www.nature.com/reprints.

https://doi.org/10.1038/s41591-026-04704-z



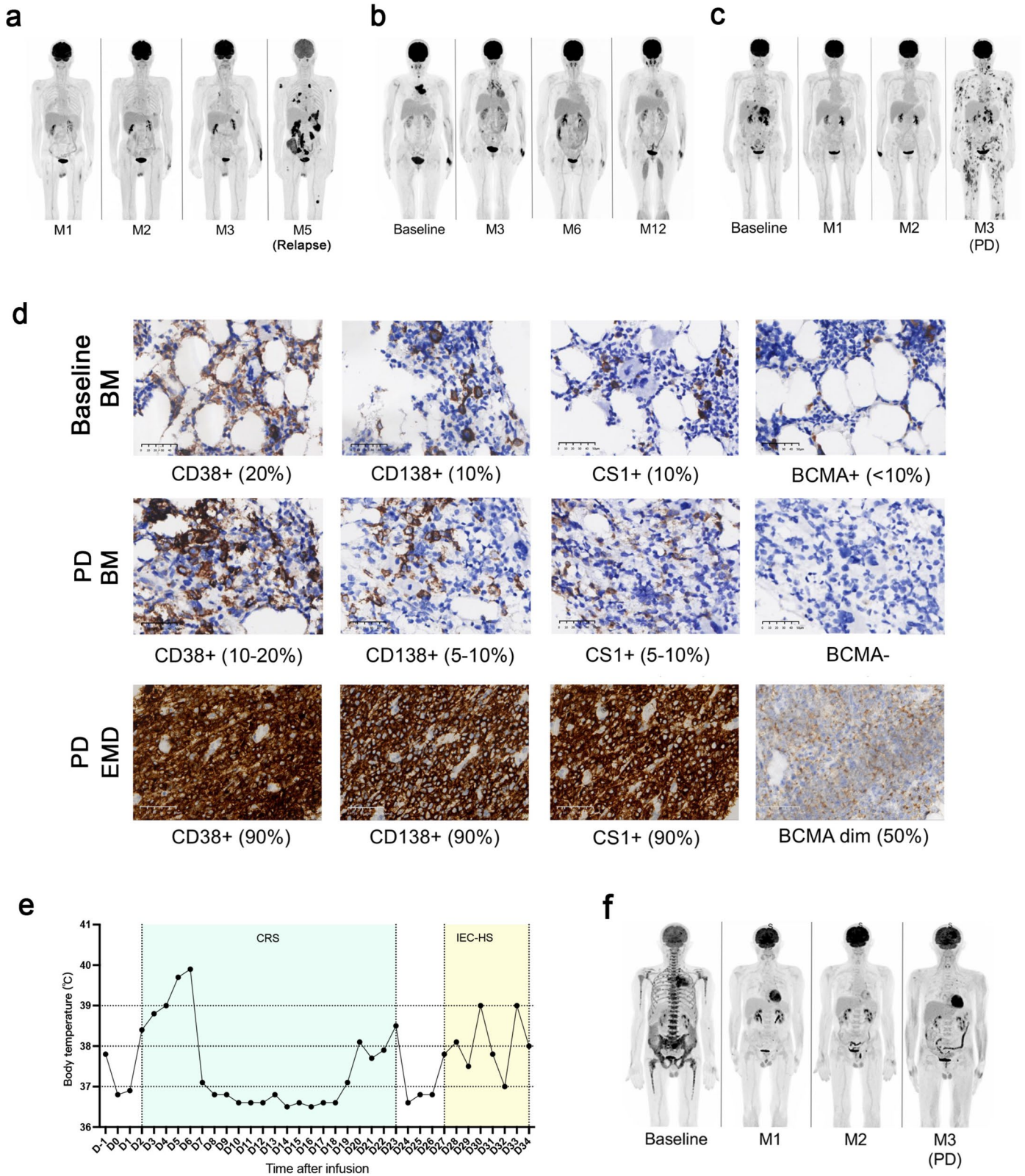
Extended Data Fig. 1 | Overview of adverse events management. (**a**) Management of adverse events following the treatment of ESO-T01. (**b**) Management of adverse events after Ex Vivo BCMA-GPRC5D CAR-T.

https://doi.org/10.1038/s41591-026-04704-z



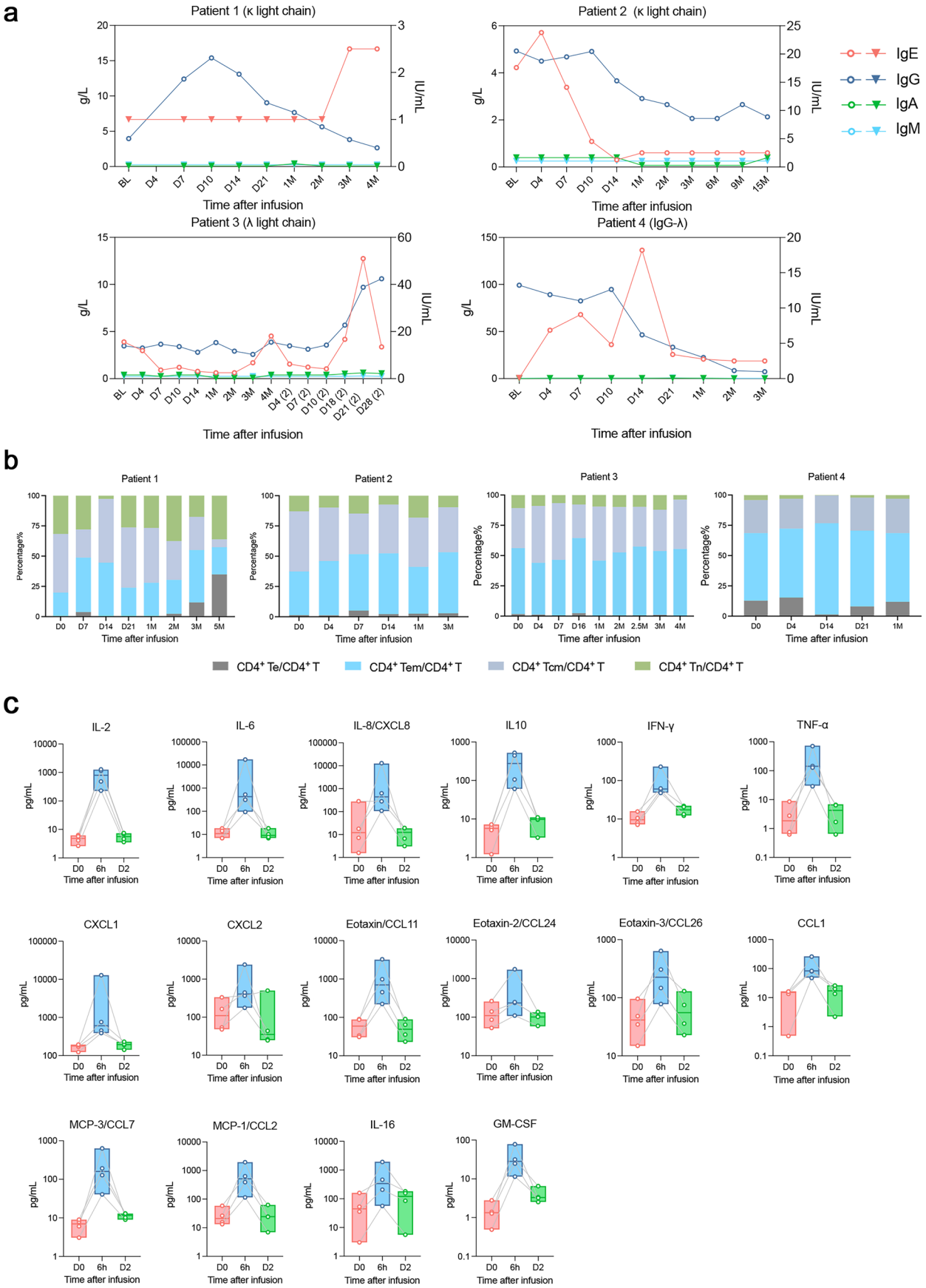
Extended Data Fig. 2 | Detection of CAR-T cells by flow cytometry in cerebrospinal fluid samples from patient 4 at months 1, 2, and 3. The CAR-T cells remained detectable until month 3.

https://doi.org/10.1038/s41591-026-04704-z



Extended Data Fig. 3 | Clinical outcomes of 4 patients. (**a**) Patient 1 achieved sCR at month 2 but relapsed by month 5. PET-CT at month 5 showed multiple hypermetabolic intramedullary and extramedullary lesions. (**b**) Patient 2 maintained sustained sCR during the follow-up. The increased metabolism in mediastinal region on the 3-month PET-CT was due to lymphnoditis. This plot only displays up to her latest PET-CT (12 M). (**c**) Patient 3 achieved PR at month 1 with marked shrinkage of extramedullary disease, but progressed at month 3 with widespread new lesions. (**d**) Immunohistochemistry of bone marrow and the new extramedullary lesion (located in the left posterior lumbar subcutaneous tissue) from patient 3, shown at baseline and at disease progression following ESO-T01 infusion. The panels display longitudinal changes across three independent clinical specimens: baseline BM, PD BM, and PD EMD (new lesion). Representative images are shown. (**e**) The changes in body temperature in patient 3 after the infusion of Ex Vivo BCMA-GPRC5D CAR-T. (**f**) Patient 4 achieved PR at month 1 but progressed at month 3, evidenced by hypermetabolic lesions in the bilateral proximal humeri and femora, as well as a pleural lesion with elevated uptake along the left 4th–6th ribs. sCR, stringent complete response; PD, progressive disease; PET-CT, Positron Emission Tomography-Computed Tomography; PR, partial response.

https://doi.org/10.1038/s41591-026-04704-z

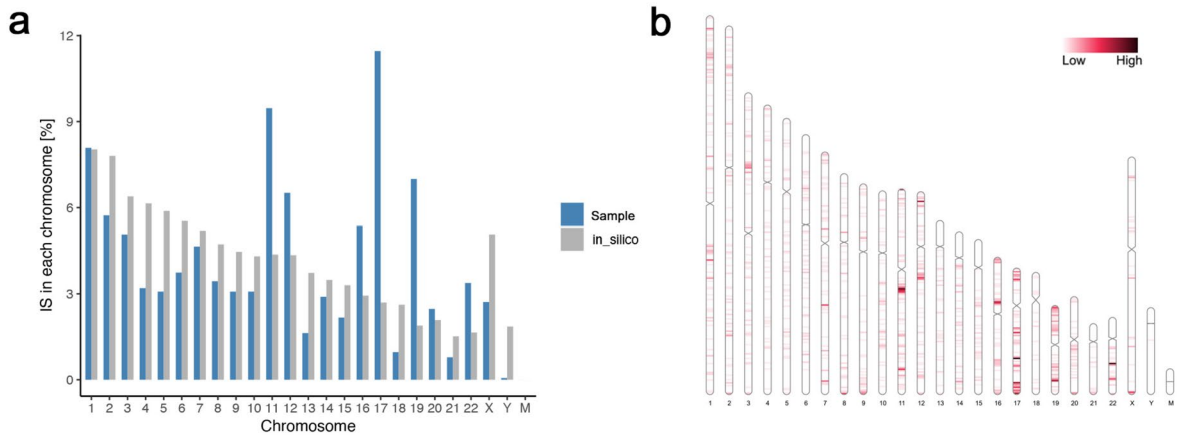


Extended Data Fig. 4 | See next page for caption.

https://doi.org/10.1038/s41591-026-04704-z

Extended Data Fig. 4 | Longitudinal immune profiling of patients following In Vivo CAR-T therapy. (**a**) Changes in immunoglobulins in 4 patients after ESO-T01 infusion. The inverted triangle indicates values of the lower limit of detection. IgG, IgA, and IgM use the left Y-axis, while IgE uses the right Y-axis. (**b**) Longitudinal profiling of $CD4^+$ T-cell immunophenotypes in 4 patients by flow cytometry. (**c**) Changes in serum cytokines and chemokines before and after In Vivo CAR-T infusion at different time points (D0 means baseline before the infusion, 6 h means 6 h post-infusion, D2 means 2 days post-infusion). Data are shown from 4 patients, and each data point represents one individual patient. No technical replicates were performed; each value is derived from a single measurement per patient sample. Data are presented as box plots where the horizontal line represents the median, and the bars extend from the minimum to the maximum values. Te, effector T cell; Tem, effector memory T cell; Tcm, central memory T cell; Tn, naive T cell.

https://doi.org/10.1038/s41591-026-04704-z



Extended Data Fig. 5 | Integration site analysis of samples from 4 patients at the expansion peak following ESO-T01 infusion. (**a**-**b**) Distribution of integration sites across different chromosomes. IS, integration site.(**a**) Bar chart comparing the distribution of IS across chromosomes between the samples (blue) and in silico prediction (gray). The y-axis represents the percentage of IS in each chromosome. (**b**) Chromosome ideograms showing the physical distribution of IS across the genome. The color scale indicates the density of IS (Low to High).

nature portfolio

Corresponding author(s): Heng Mei

Last updated by author(s): Aug 21, 2026

Reporting Summary

Nature Portfolio wishes to improve the reproducibility of the work that we publish. This form provides structure for consistency and transparency in reporting. For further information on Nature Portfolio policies, see our Editorial Policies and the Editorial Policy Checklist.

Statistics

For all statistical analyses, confirm that the following items are present in the figure legend, table legend, main text, or Methods section.

n/a	Confirmed
☐	☒ The exact sample size (*n*) for each experimental group/condition, given as a discrete number and unit of measurement
☒	☐ A statement on whether measurements were taken from distinct samples or whether the same sample was measured repeatedly
☒	☐ The statistical test(s) used AND whether they are one- or two-sided *Only common tests should be described solely by name; describe more complex techniques in the Methods section.*
☒	☐ A description of all covariates tested
☒	☐ A description of any assumptions or corrections, such as tests of normality and adjustment for multiple comparisons
☒	☐ A full description of the statistical parameters including central tendency (e.g. means) or other basic estimates (e.g. regression coefficient) AND variation (e.g. standard deviation) or associated estimates of uncertainty (e.g. confidence intervals)
☒	☐ For null hypothesis testing, the test statistic (e.g. *F*, *t*, *r*) with confidence intervals, effect sizes, degrees of freedom and *P* value noted *Give P values as exact values whenever suitable.*
☒	☐ For Bayesian analysis, information on the choice of priors and Markov chain Monte Carlo settings
☒	☐ For hierarchical and complex designs, identification of the appropriate level for tests and full reporting of outcomes
☒	☐ Estimates of effect sizes (e.g. Cohen's *d*, Pearson's *r*), indicating how they were calculated

Our web collection on statistics for biologists contains articles on many of the points above.

Software and code

Policy information about availability of computer code

Data collection	Bio-Rad CFX96 System, BD FACSymphony A1 (BD, USA), LUMINEX 200 instrument, Qubit 4.0, TapeStation 4150, MiSeq platform (Illumina), and Titan automated stainer (Maixin Biotech, Fuzhou, China).
Data analysis	FlowJo v.10.6.1, Genome Integration Site Analysis pipeline (GENE-IS), QuPath v.0.4.3, and Graph Pad Prism v.10.4.1.

For manuscripts utilizing custom algorithms or software that are central to the research but not yet described in published literature, software must be made available to editors and reviewers. We strongly encourage code deposition in a community repository (e.g. GitHub). See the Nature Portfolio guidelines for submitting code & software for further information.

Data

Policy information about availability of data

All manuscripts must include a data availability statement. This statement should provide the following information, where applicable:

- Accession codes, unique identifiers, or web links for publicly available datasets
- A description of any restrictions on data availability
- For clinical datasets or third party data, please ensure that the statement adheres to our policy

All primary data are included in this article and its supplementary materials, which provide patient-level details on safety, response, pharmacokinetics, immunophenotyping, vector constructs, integration sites, and gating strategies. Individual-level clinical datasets are not publicly available for proprietary and privacy reasons but have been de-identified and stored securely at Wuhan Union Hospital. Access may be granted to qualified researchers upon request to the

corresponding author. Applicants must sign a data-use agreement defining the research scope, and commercial use is prohibited. After approvals from both the applicant's institution and our internal data access committee, de-identified data will be delivered within 6 months of publication. The full protocol and statistical analysis plan are provided online. Requests should be sent to hmei@hust.edu.cn. Responses will be given within 10 working days. The full trial protocol and the statistical analysis plan are provided in the supplementary materials.

Research involving human participants, their data, or biological material

Policy information about studies with human participants or human data. See also policy information about sex, gender (identity/presentation), and sexual orientation and race, ethnicity and racism.

Reporting on sex and gender	Sex was assessed via participant self-report. Due to the small size of the cohort, neither sex nor gender was specifically considered in the enrollment criteria, and disaggregated analysis by sex was not performed.
Reporting on race, ethnicity, or other socially relevant groupings	Not applicable.
Population characteristics	We evaluate biological sex, age at CAR-T infusion, ethnicity, oncological history, disease risk, exposure to prior therapy, and the characteristics of infused CAR-T and expanded CAR-T cells.
Recruitment	We retrospectively report data from four patients who received In Vivo CAR-T therapy (ESO-T01) for relapsed or refractory multiple myeloma at Wuhan Union Hospital and underwent follow-up between November 2024 and March 2026.
Ethics oversight	The study was approved by the Ethics Committee of the Union Hospital affiliated to Huazhong University of Science and Technology, Wuhan, China, and all subjects provided informed consent (REC ref no. [2024] 0915-02).

Note that full information on the approval of the study protocol must also be provided in the manuscript.

Field-specific reporting

Please select the one below that is the best fit for your research. If you are not sure, read the appropriate sections before making your selection.

☒ Life sciences ☐ Behavioural & social sciences ☐ Ecological, evolutionary & environmental sciences

For a reference copy of the document with all sections, see nature.com/documents/nr-reporting-summary-flat.pdf

Life sciences study design

All studies must disclose on these points even when the disclosure is negative.

Sample size	From November 2024 to February 2025, six patients with R/R MM underwent screening. Two individuals were excluded: one failed to meet the disease progression criteria, and the other lacked measurable disease. Four patients were eventually enrolled and treated with ESO-T01.
Data exclusions	Not applicable.
Replication	Not applicable. The analyses were performed on unique samples during clinical investigation.
Randomization	Not applicable.
Blinding	Not applicable. Blinding was not relevant to this single-arm study, as there was no control group and all participants received the same intervention.

Reporting for specific materials, systems and methods

We require information from authors about some types of materials, experimental systems and methods used in many studies. Here, indicate whether each material, system or method listed is relevant to your study. If you are not sure if a list item applies to your research, read the appropriate section before selecting a response.

Materials & experimental systems

n/a	Involved in the study
☐	☒ Antibodies
☐	☒ Eukaryotic cell lines
☒	☐ Palaeontology and archaeology
☒	☐ Animals and other organisms
☐	☒ Clinical data
☒	☐ Dual use research of concern
☒	☐ Plants

Methods

n/a	Involved in the study
☒	☐ ChIP-seq
☐	☒ Flow cytometry
☒	☐ MRI-based neuroimaging

Antibodies

Antibodies used

CD3-APC (317317; Biolegend), PE-streptavidin (405204; Biolegend), Fixable Viability Stain 780 (565388; BD Horizon), CD3-Percp5.5(317336; Biolegend), CD4-FITC (980802; Biolegend), CD8-PE-Cy7 (344712; Biolegend), CD45RA-APC (304112; Biolegend), CD62L-BV510 (304843; Biolegend), CD28-BV605 (562976; BD Horizon), and CD57-PE594 (562488; BD Horizon) for flow cytometry. CD38(303502; Biolegend), CD138 (356501; Biolegend); CSI (HY-P84817A; MedChemExpress), BCMA(NBP1-97637; R&D Systems) for immunohistochemistry. Flow?cytometry antibodies were used at 2.0 µL per test and are listed with their respective markers, fluorophores, manufacturers, and catalog numbers. Antibodies for IHC were applied at a dilution of 1:1000.

Validation

For each of the antibody used is provided the catalog number to access the provider company with the specific references for validation.
CD3-APC (317317; Biolegend): Song C, et al. 2022. Stem Cell Res Ther. 13:48.
PE-streptavidin (405204; Biolegend): Cao Y, et al. 2023. Nature. 614:521.
Fixable Viability Stain 780 (565388; BD Horizon): Gonzalez Lopez M et al. 2026. Nat Commun. 17;17(1):6537.
CD3-Percp5.5(317336; Biolegend): Kaku CI, et al. 2023. Nat Commun. 14:2751.
CD4-FITC (980802; Biolegend): Xu J, et al. 2025. Lancet. 406(10500):228-231.
CD8-PE-Cy7 (344712; Biolegend): Battistello E, et al. 2023. Mol Cell. 83:1216.
CD45RA-APC (304112; Biolegend): Cox MJ, et al. 2022. Leukemia. 36:1635.
CD62L-BV510 (304843; Biolegend): Bonifacius A, et al. 2021. Immunity. 54(2):340-354.e6.
CD28-BV605 (562976; BD Horizon): Ramgopal, M. N. et al. 2025. Nat Med. 31(11):3879-3888.
CD57-PE594 (562488; BD Horizon): Board, N. L. et al. 2024. Nat Immunol. 25, 462–470
CD38 303502; Biolegend): Roukens AHE, et al. 2022. Nat Immunol. 23:23.
CD138 (356501; Biolegend): Nerreter T, et al. 2019. Nat Commun. 10:3137.
CSI (HY-P84817A; MedChemExpress): Li C, et al. 2024. Leukemia. 38(1):149-159.
BCMA(NBP1-97637; R&D Systems) : Geis M et al. 2021. Commun Biol. 8;4(1):44

Eukaryotic cell lines

Policy information about cell lines and Sex and Gender in Research

Cell line source(s)

CHO cells were obtained from the American Type Culture Collection (ATCC, Manassas, VA, USA; catalog No. CCL-61).

Authentication

Cell lines were periodically authenticated through Sangon Biotech.

Mycoplasma contamination

All cell lines tested negative for mycoplasma.

Commonly misidentified lines
(See ICLAC register)

None.

Clinical data

Policy information about clinical studies

All manuscripts should comply with the ICMJE guidelines for publication of clinical research and a completed CONSORT checklist must be included with all submissions.

Clinical trial registration

The NCT number is NCT06691685. This clinical trial is registered with ClinicalTrials.gov.

Study protocol

This phase I, single-arm, open-label study was conducted at Wuhan Union Hospital, Huazhong University of Science and Technology, China. The aim was to evaluate the safety, tolerability, and preliminary efficacy of ESO-T01, a third-generation, non-replicating, self-inactivating lentiviral vector encoding anti-BCMA CAR, in patients with R/R MM. This study was approved by the Ethics Committee of the Union Hospital affiliated to Huazhong University of Science and Technology, Wuhan, China (REC ref no. [2024]0915-02). The study was registered in ClinicalTrials.gov (NCT06691685) on November 9, 2024. Due to the acquisition of the sponsor, EsoBiotec, by AstraZeneca, the study was terminated, and no more patients were enrolled.
The protocol was once amended to allow prophylactic use of glucocorticoid before infusion, to include patients who suffered from clinical relapse (including new bone lesions or confirmed increase [≥50% increase in SPD of measurable lesions with an absolute value of ≥ 1 cm] of lesions or soft?tissue plasmacytomas), to specify that urine protein electrophoresis, urine immunofixation electrophoresis, and urine free light chain assessments are performed on 24?hour urine collections; and to accept test results obtained within 7 days before screening as valid screening data. The protocol accompanying our previously published report was the

	amended version. The complete study protocol has been provided as an attachment to the article.
Data collection	Data was collected from November 2024 to March 2026.
Outcomes	We update the data on long term safety and response durability with a maximal follow up of 15 months. No immunogenicity or integration related toxicities occurred, and no important adverse events related to ESO-T01 emerged beyond the initial report. Of four patients, one maintained sCR for 15 months. Three patients relapsed or progressed, all with extramedullary involvement, and eventually died during follow-up. The median progression-free survival was 4.0 (range, 3.0-15.0) months.

Plants

Seed stocks	n/a
Novel plant genotypes	n/a
Authentication	n/a

Flow Cytometry

Plots

Confirm that:

☒ The axis labels state the marker and fluorochrome used (e.g. CD4-FITC).

☒ The axis scales are clearly visible. Include numbers along axes only for bottom left plot of group (a 'group' is an analysis of identical markers).

☒ All plots are contour plots with outliers or pseudocolor plots.

☒ A numerical value for number of cells or percentage (with statistics) is provided.

Methodology

Sample preparation	Peripheral blood and cerebrospinal fluid samples from patients were analyzed using flow cytometry to assess the characteristics of CAR-T cells and their subsets. Details are provided for each specific experiment in the method section.
Instrument	BD FACSymphony A1 (BD, USA)
Software	BD FACSDiva software (BD Bioscience), and analyzed by FlowJo v.10.6.1.
Cell population abundance	Typically, 0.5-1 x 10^6 PBMCs were stained per timepoint.
Gating strategy	Singlets were gated, followed by live cells, lymphocytes, and then CD3+T subset. Analysis was performed on CD3+T cells including CAR-positive populations. Counting beads were also gated.

☒ Tick this box to confirm that a figure exemplifying the gating strategy is provided in the Supplementary Information.